S-matrix equivalence theorem evasion and dimensional regularisation with the canonical MHV lagrangian

James H. Ettle,[a] **Chih-Hao Fu,**[b] **Jonathan P. Fudger,**[a] **Paul R.W. Mansfield**[b] **and Tim R. Morris**[a]

[a] *School of Physics and Astronomy, University of Southampton*
Highfield, Southampton, SO17 1BJ, U.K.
[b] *Department of Mathematical Sciences, University of Durham*
South Road, Durham, DH1 3LE, U.K.
E-mail: jhe@phys.soton.ac.uk, chih-hao.fu@durham.ac.uk,
j.p.fudger@phys.soton.ac.uk, P.R.W.Mansfield@durham.ac.uk,
T.R.Morris@soton.ac.uk

ABSTRACT: We demonstrate that the canonical change of variables that yields the MHV lagrangian, also provides contributions to scattering amplitudes that evade the equivalence theorem. This 'ET evasion' in particular provides the tree-level $(-++)$ amplitude, which is non-vanishing off shell, or on shell with complex momenta or in $(2,2)$ signature, and is missing from the MHV (a.k.a. CSW) rules. At one loop there are ET-evading diagrammatic contributions to the amplitudes with all positive helicities. We supply the necessary regularisation in order to define these contributions (and quantum MHV methods in general) by starting from the light-cone Yang-Mills lagrangian in D dimensions and making a canonical change of variables for all $D-2$ transverse degrees of freedom of the gauge field. In this way, we obtain dimensionally regularised three- and four-point MHV amplitudes. Returning to the one-loop $(++++)$ amplitude, we demonstrate that its quadruple cut coincides with the known result, and show how the original light-cone Yang-Mills contributions can in fact be algebraically recovered from the ET-evading contributions. We conclude that the canonical MHV lagrangian, supplemented with the extra terms brought to correlation functions by the non-linear field transformation, provide contributions which are just a rearrangement of those from light-cone Yang-Mills and thus coincide with them both on and off shell.

KEYWORDS: QCD, Gauge Symmetry.

Contents

1. Introduction

Much recent activity in perturbative QCD has revolved around a variety of new techniques for calculating Yang-Mills scattering amplitudes that have considerable computational advantages over the traditional Feynman graph approach.

Parke and Taylor obtained very compact expressions for the MHV (and $\overline{\text{MHV}}$) amplitudes [1–3], which were found to have a simple geometrical interpretation in twistor space [4]. Taking inspiration from twistor-string theory, Cachazo, Svrček and Witten formulated the MHV rules (or CSW rules) [5] for the construction of tree-level scattering amplitudes. These rules treat MHV amplitudes as vertices, and continue them off-shell by a particular prescription. The vertices are joined by scalar propagators. These rules have

since seen extensive application (e.g. in [6–11]) and have been proved a number of ways (such as [12] and [13]). Britto, Cachazo, Feng and Witten [12, 14, 15] discovered recursion relations between on-shell tree-level scattering amplitudes (the so-called BCFW approach) that ultimately reduce everything to sums of products of the MHV and $\overline{\text{MHV}}$ amplitudes.

These methods have not been as forthcoming for quantum-level computations. Nevertheless, considerable ingenuity has yielded several results for perturbative Yang-Mills at one-loop (including amplitudes with any number of gluons where at most two gluons have a different helicity to the others [16–19], and certain configurations for up seven gluons [20, 21]) by application of unitarity, generalised unitarity and cut construction [22, 23], on-shell recursion relations/bootstrapping [18, 21, 24–26], the holomorphic anomaly [20, 27–29], using the CSW rules within loops, evaluating the diagrams with the Feynman tree theorem [30, 31], and hybrid techniques extracting the rational pieces from the Feynman diagrams [32]. Being entirely cut-constructable, $\mathcal{N} = 1$ and $\mathcal{N} = 4$ SYM are particularly amenable to generalised unitarity approaches, examples of which can be found in [30, 33–40]. Indeed, Yang-Mills amplitudes can be written as a linear combination of $\mathcal{N} = 1$ and $\mathcal{N} = 4$ pieces, leaving a scalar loop [23, 33]. The latter may be evaluated using the methods discussed above, including novel approaches to generalised unitarity outside four dimensions that recover the rational parts [23]. Nevertheless, a systematic, tractable approach to calculating *complete* one-loop amplitudes with MHV techniques is yet to be found.

The CSW approach applied at the tree and quantum level, is highly suggestive of a quantum field theory, but up until recently it was not formulated in the lagrangian framework which would allow us to use the full machinery of quantum field theory; instead it has been supported by conjecture, demonstration and varying degrees of proof. Progress of particular interest to the work herein was presented in refs. [41] and [42], where a *canonical* transformation of the field variables was described that mapped the self-dual sector of Yang-Mills on to [the kinetic term of] a free field theory. Doing so resulted in a lagrangian with an infinite set of terms, each forming an MHV vertex. These vertices would be joined by scalar propagators following the CSW prescription; that scattering amplitudes calculated with the new vertices matched the traditional results at tree-level followed providing the equivalence theorem [43, 45] was satisfied. This transformation was made explicit in [46] where it was demonstrated that the terms were MHV vertices (for up to five gluons).

In the meantime, other developments invoking similar techniques driven by field transformation have arisen. Feng and Huang [47] obtained an MHV lagrangian for $\mathcal{N} = 4$ Super-Yang-Mills in light-cone superspace by a change of the superfield variables. Brandhuber, Spence and Travaglini [48] consider just a holomorphic change of variables, arguing that the one-loop all-+ amplitude then arises from the transformation's jacobian. Boels, Mason and Skinner [49–52] recover MHV diagrams using a twistor action with which they show that the formalism arises from a gauge transformation on the larger twistor space (as opposed to a non-linear field redefinition).

In this paper, we develop the ideas of [42, 46]. We have already noted there that the treatment of the canonical MHV lagrangian at the quantum level required proper

regulation, and that certain amplitudes known not to vanish could not be constructed from its vertices. Here, we demonstrate that the missing amplitudes arise naturally from application of the standard procedure of LSZ reduction [45] to the theory's correlation functions, in this case leaving behind evasions of the equivalence theorem. We incorporate dimensional regularisation by applying the canonical transformation to all the transverse degrees of freedom of light-cone Yang-Mills (henceforth LCYM) in $D = 4 - 2\epsilon$ dimensions. This is then used to investigate the four-gluon all-+ amplitude.

In section 2, we review the construction of the canonical MHV lagrangian in four dimensions. We show how the construction evades the equivalence theorem in section 3, and use this to recover the $(-++)$ amplitude. This is non-vanishing on shell with complex momenta or in $(2, 2)$ signature but we see that we recover the three-point $\overline{\text{MHV}}$ amplitude even off shell with the appropriate CSW prescription.

Section 4 derives the canonical MHV lagrangian in D dimensions. We obtain the series coefficients that specify the change of variables and the appropriate generalisations of the three- and four-point MHV amplitudes. We note that the series coefficients can be written in terms of the three-point $\overline{\text{MHV}}$ vertex that was eliminated in the canonical transformation, emphasising the generality of this procedure. This step helps clarify how the missing amplitudes are recovered, which we do in the next section.

We then analyse the one-loop $(++++)$ amplitude. We show that at the algebraic level, i.e. before taking on-shell limits or performing the loop integral, that the ET-evading contributions sum up to precisely the missing amplitudes that LCYM would have provided. We concentrate on the LCYM box contribution, which we uncover by tracing the momentum routing through the three-point $\overline{\text{MHV}}$ vertices. Although we concentrate on this one topology it is clear that all the LCYM contributions are recovered in this way.

We also analyse cuts of the ET-evading contributions, demonstrating that the quadruple cut of the propagators coincides with that of the known one-loop $(++++)$ amplitude. This serves also to show that our off shell D dimensional generalisations of the spinor bracket techniques can be used efficiently to compute these amplitudes.

Finally in section 6 we draw all these strands together, make our conclusions, and indicate directions for future research.

2. A review of the 4D canonical MHV lagrangian

In this section, we will briefly review the canonical MHV lagrangian in four dimensions. This will also serve to explain the conventions we use for this paper.

2.1 Light-cone co-ordinates

The construction of the canonical MHV lagrangian discussed in [42] begins with LCYM theory [53] in a co-ordinate system defined by

$$x^0 = \frac{1}{\sqrt{2}}(t - x^3), \quad x^{\bar{0}} = \frac{1}{\sqrt{2}}(t + x^3), \quad z = \frac{1}{\sqrt{2}}(x^1 + ix^2), \quad \bar{z} = \frac{1}{\sqrt{2}}(x^1 - ix^2). \quad (2.1)$$

Note here the presence of the $1/\sqrt{2}$ factors that preserve the normalisation of the volume form. It useful to employ a compact notation for the components of 1-forms in these

co-ordinates, for which we write $(p_0, p_{\bar{0}}, p_z, p_{\bar{z}}) \equiv (\check{p}, \hat{p}, p, \bar{p})$; for momenta labelled by a number, we write that number with a decoration, for example the nth external momentum has components $(\check{n}, \hat{n}, \tilde{n}, \bar{n})$. In these co-ordinates and with this notation, the Lorentz invariant reads

$$A \cdot B = \check{A}\hat{B} + \hat{A}\check{B} - A\bar{B} - \bar{A}B. \tag{2.2}$$

The following bilinears are also defined:

$$(1\,2) := \hat{1}\tilde{2} - \hat{2}\tilde{1}, \quad \{1\,2\} := \hat{1}\bar{2} - \hat{2}\bar{1}. \tag{2.3}$$

In four dimensions, we can express these bilinears in terms of the conventional angle and square brackets often found in the literature. We will not make much use of the spinor formalism in this paper, but it is nevertheless illuminating to consider this relationship. Begin by noting that for a 4-vector p, its bispinor representation is

$$(p_{\alpha\dot{\alpha}}) = \sqrt{2}\begin{pmatrix} \check{p} & -p \\ -\bar{p} & \hat{p} \end{pmatrix},$$

and that for null p this factors into $p_{\alpha\dot{\alpha}} = \lambda_\alpha\tilde{\lambda}_{\dot{\alpha}}$ where we can choose

$$\lambda = 2^{1/4}\begin{pmatrix} -p/\sqrt{\hat{p}} \\ \sqrt{\hat{p}} \end{pmatrix} \quad \text{and} \quad \tilde{\lambda} = 2^{1/4}\begin{pmatrix} -\bar{p}/\sqrt{\hat{p}} \\ \sqrt{\hat{p}} \end{pmatrix}. \tag{2.4}$$

Hence the spinor brackets can be expressed as

$$\langle 1\,2 \rangle := \epsilon^{\alpha\beta}\lambda_{1\alpha}\lambda_{2\beta} = \sqrt{2}\frac{(1\,2)}{\sqrt{\hat{1}\hat{2}}} \quad \text{and} \quad [1\,2] := \epsilon^{\dot{\alpha}\dot{\beta}}\lambda_{1\dot{\alpha}}\lambda_{2\dot{\beta}} = \sqrt{2}\frac{\{1\,2\}}{\sqrt{\hat{1}\hat{2}}}. \tag{2.5}$$

Observe that λ and $\tilde{\lambda}$ shown in (2.4) are also defined for non-null p. In this case, their product corresponds to the null vector

$$\lambda\tilde{\lambda} = p + a\mu, \tag{2.6}$$

where $\mu = \eta\tilde{\eta} = (1,0,0,1)/\sqrt{2}$ in Minkowski co-ordinates is the null vector normal to surfaces of constant x^0, and a is a coefficient which is unimportant here. By contracting both sides of (2.6) with $\tilde{\eta}$, we see that λ satisfies the CSW prescription [5] for continuing spinor momenta off the mass shell.
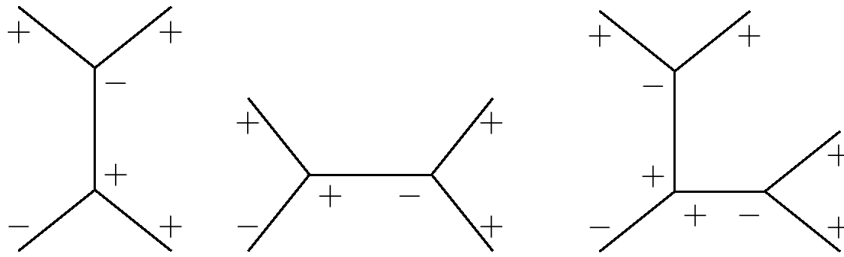
2.2 The field transformation

The Yang-Mills action can be written as

$$S = \frac{1}{2g^2}\int d^4x\, \text{tr}\mathcal{F}^{\mu\nu}\mathcal{F}_{\mu\nu},$$

where d^4x is the Minkowski volume element and we define the field-strength tensor $\mathcal{F}$ by

$$\mathcal{F}_{\mu\nu} = [D_\mu, D_\nu], \quad D_\mu = \partial_\mu + \mathcal{A}_\mu, \quad \mathcal{A}_\mu = -\frac{ig}{\sqrt{2}}A_\mu^a T^a. \tag{2.7}$$

Figure 1: Examples of possible tree-level diagrams that can be constructed from the Chalmers-Siegel truncation of LCYM.

Our internal group generators are normalised according to the convention of [56] as

$$[T^a, T^b] = i\sqrt{2}f^{abc}T^c, \quad \text{tr}(T^aT^b) = \delta^{ab}. \tag{2.8}$$

Quantisation takes place on surfaces Σ of constant x^0 with normal μ defined as above. We choose the axial gauge condition $\mu \cdot \mathcal{A} = \hat{\mathcal{A}} = 0$, for which the Faddeev-Popov ghosts are completely decoupled. The lagrangian density is then quadratic in the $\check{\mathcal{A}}$ field, and we integrate it out of the partition function to obtain the light-cone action

$$S = \frac{4}{g^2} \int dx^0 \, (L^{-+} + L^{-++} + L^{--+} + L^{'--++}), \tag{2.9}$$

where

$$L^{-+} = \quad \text{tr} \int_{\Sigma} d^3\mathbf{x} \, \bar{\mathcal{A}}(\check{\partial}\hat{\partial} - \partial\bar{\partial})\mathcal{A} \tag{2.10}$$

$$L^{-++} = -\text{tr} \int_{\Sigma} d^3\mathbf{x} \, (\bar{\partial}\hat{\partial}^{-1}\mathcal{A}) \, [\mathcal{A}, \hat{\partial}\bar{\mathcal{A}}] \tag{2.11}$$

$$L^{--+} = -\text{tr} \int_{\Sigma} d^3\mathbf{x} \, [\bar{A}, \hat{\partial}\mathcal{A}] \, (\partial\hat{\partial}^{-1}\bar{\mathcal{A}}) \tag{2.12}$$

$$L^{'--++} = -\text{tr} \int_{\Sigma} d^3\mathbf{x} \, [\bar{A}, \hat{\partial}\mathcal{A}] \, \hat{\partial}^{-2} \, [\mathcal{A}, \hat{\partial}\bar{\mathcal{A}}]. \tag{2.13}$$

The unwanted L^{-++} is removed by defining a new Lie algebra valued field $\mathcal{B}$ such that

$$L^{-+}[\mathcal{A}] + L^{-++}[\mathcal{A}] = L^{-+}[\mathcal{B}]. \tag{2.14}$$

It may seem rather perverse to absorb the three-point $-++$ vertex into the kinetic term, as in (2.14). It makes sense once one recognises that the left hand side is the self-dual sector of Yang-Mills [44] which at tree level gives only diagrams with one negative helicity and all the rest positive, as illustrated in figure 1. Such terms are well known to vanish on shell [56], so at least in four dimensions, and at tree level and on shell, we are simply making explicit what is already a free theory. We will reconsider this point in more generality in the conclusions.

The transformation is performed entirely on the quantisation surface Σ, and so all the fields have the same x^0 dependence, which we suppress. By restricting $\mathcal{A}$ to be a function of $\mathcal{B}$ alone and requiring the transformation to be canonical, we find that $\bar{\mathcal{A}}$ must be a function of $\mathcal{B}$ and $\bar{\mathcal{B}}$, and contain only one power of the latter. Now working in momentum space on Σ, we can write the following series solutions:

$$\mathcal{A}_1 = \sum_{n=2}^{\infty} \int_{2\cdots n} \Upsilon(1\cdots n)\, \mathcal{B}_{\bar{2}} \cdots \mathcal{B}_{\bar{n}}\, (2\pi)^3 \delta(\textstyle\sum_{i=1}^{n} \mathbf{p}_i), \tag{2.15}$$

$$\hat{1}\bar{\mathcal{A}}_{\bar{1}} = \sum_{m=2}^{\infty} \sum_{s=2}^{m} \int_{2\cdots m} \hat{s}\, \Xi^{s-1}(\bar{1}2\cdots m)\, \mathcal{B}_{\bar{2}} \cdots \bar{\mathcal{B}}_{\bar{s}} \cdots \mathcal{B}_{\bar{m}}\, (2\pi)^3 \delta(\textstyle\sum_{i=1}^{m} \mathbf{p}_i), \tag{2.16}$$

where $\Upsilon(12) = \Xi^1(12) = 1$. Note that the numbered subscripts above are momentum arguments, and the bar implies negation: $\mathcal{B}_{\bar{i}} := \mathcal{B}(-\mathbf{p}_i)$. The integral short-hand here is defined by

$$\int_{1\cdots n} \equiv \prod_{k=1}^{n} \frac{1}{(2\pi)^3} \int d\hat{k}\, dk\, d\bar{k}.$$

The requirement that the transformation is canonical and (2.14) imply the following recursion relations for Υ and Ξ:

$$\Upsilon(1\cdots n) = \frac{i}{\omega_1 + \cdots + \omega_n} \sum_{j=2}^{n-1} (\zeta_{j+1,n} - \zeta_{2,j}) \Upsilon(-,2,\cdots,j) \Upsilon(-,j+1,\cdots,n), \tag{2.17}$$

$$\Xi^l(1\cdots n) = - \sum_{r=\max(2,4-l)}^{n+1-l} \sum_{m=\max(r,3)}^{r+l-1} \Upsilon(-,n-r+3,\cdots,m-r+1) \tag{2.18}$$
$$\times\, \Xi^{l+r-m}(-,m-r+2,\cdots,n-r+2).$$

Here, and hereafter, the arguments labelled "$-$" are minus the sum of the remaining arguments (as follows from momentum conservation), $\zeta_{j,k} := \zeta(\sum_{i=j}^{k} p_i)$ where $\zeta(p) := \bar{p}/\hat{p}$, $\omega_j = \tilde{j}\bar{j}/\hat{j}$, and momentum indices must be interpreted cyclically. These can be solved to give[1]

$$\Upsilon(1\cdots n) = i^n \frac{\hat{1}\hat{3}\cdots\widehat{n-1}}{(2\,3)\cdots(n-1,n)}, \tag{2.19}$$

$$\Xi(1\cdots n) = -\frac{\hat{s}}{\hat{1}}\Upsilon(1\cdots n). \tag{2.20}$$

Putting all this together, it is not difficult to see that the remaining pieces of the lagrangian (2.12), (2.13) are transformed into an infinite series of terms, labelled by helicity, each with two factors of $\bar{\mathcal{B}}$ such that

$$L = L^{-+}[\mathcal{B}] + L^{--+}[\mathcal{B}] + L^{--++}[\mathcal{B}] + L^{--+++}[\mathcal{B}] + \cdots. \tag{2.21}$$

Explicit substitution shows that the vertices,

$$\frac{1}{2} \sum_{s=2}^{n} \int_{1\cdots n} V^s(1\cdots n)\, \mathrm{tr}[\bar{\mathcal{B}}(-\mathbf{p}_1)\mathcal{B}(-\mathbf{p}_2)\cdots\mathcal{B}(-\mathbf{p}_s)\cdots\mathcal{B}(-\mathbf{p}_n)]\,(2\pi)^3\delta(\textstyle\sum_{i=1}^{n}\mathbf{p}_i), \tag{2.22}$$

---

[1]For $\Upsilon(123)$, in the numerator only the $\hat{1}$ is retained.

contained therein are, indeed, the MHV amplitudes.

At this point it is important to address the normalisation of the gauge fields. So far we have been working with a non-canonical normalisation from (2.9), (2.10) and (2.21) that absorbs the coupling constant and group generators; one upshot of this is that the tree-level expression for a $\mathcal{B}$ propagator is

$$\langle \mathcal{B}\bar{\mathcal{B}} \rangle = -\frac{ig^2}{2p^2}. \tag{2.23}$$

Upon substitution for fields with the canonical normalisation using (2.7), i.e. using the same transformation also for $\mathcal{B}$ and $\bar{\mathcal{B}}$, one finds of course the $B(\bar{B})$ propagator i/p^2, as expected. Particular care must therefore be taken to use the appropriate propagator (2.23) and external polarisation vectors in conjunction with the series coefficients Υ and Ξ as defined in (2.19) and (2.20). Alternatively, one can work (as we will do in the computations to follow) entirely with canonical normalisation by making the replacements

$$V^s(1\cdots n) \to \frac{4}{g^2}\left(-\frac{ig}{\sqrt{2}}\right)^n V^s(1\cdots n), \tag{2.24}$$

$$\Upsilon(1\cdots n) \to \left(-\frac{ig}{\sqrt{2}}\right)^{n-2} \Upsilon(1\cdots n), \tag{2.25}$$

$$\Xi^s(1\cdots n) \to \left(-\frac{ig}{\sqrt{2}}\right)^{n-2} \Xi^s(1\cdots n). \tag{2.26}$$

With the off-shell definitions (2.5), the vertices are then precisely the Parke-Taylor MHV amplitudes:

$$V^s(1\cdots n) = g^{n-2} \frac{\langle 1\,s \rangle^4}{\langle 1\,2 \rangle \langle 2\,3 \rangle \cdots \langle n-1, n \rangle \langle n\,1 \rangle}. \tag{2.27}$$

3. Tree-level equivalence theorem evasion

Now we have enough tools to obtain the tree-level $(-++)$ amplitude, which cannot be constructed from the vertices of the theory. We explain that this arises from a evasion of the equivalence theorem.

3.1 On LSZ reduction and scattering amplitudes

Scattering amplitudes are formed by the application of LSZ reduction to correlation functions of the A fields. For outgoing momenta $\{p_i\}$ and helicities $\{h_i\}$,

$$\langle p_1^{h_1}, \ldots, p_n^{h_n}|S|0 \rangle = (-i)^n \lim_{p_i^2 \to 0} p_1^2 \cdots p_n^2 \, \langle E_{h_1}^{\mu_1} A_{\mu_1} \cdots E_{h_n}^{\mu_n} A_{\mu_n} \rangle. \tag{3.1}$$

The $E_{h_i}^{\mu_i}$ are polarisation vectors in four dimensions using the outgoing helicity convention, hence no complex conjugation. The polarisations are given (in the spinor helicity formalism) by

$$E_+ = \sqrt{2}\frac{\eta\,\tilde{\lambda}}{\langle \eta\,\lambda \rangle} \quad \text{and} \quad E_- = \sqrt{2}\frac{\lambda\,\tilde{\eta}}{[\eta\,\lambda]} \tag{3.2}$$

Figure 2: The MHV completion vertices: graphical representations of the Υ and Ξ coefficients of the series expansion of $\mathcal{A}$ and $\bar{\mathcal{A}}$ (shown up to $\mathcal{O}(\mathcal{B}^2)$). The wavy lines with a $+(-)$ denote insertions of $\mathcal{A}(\bar{\mathcal{A}})$ operators in correlation functions; $\mathcal{B}$ and $\bar{\mathcal{B}}$ attach to the straight lines.

where (up to an unimportant phase) η and $\tilde{\eta}$ are defined as below (2.5). Then $E_+ = \bar{E}_- = -1$, and by considering the invariant (2.2), we see that each $+(-)$ external state gluon on the left-hand side of (3.1) is associated with an $\bar{A}(A)$ field in the correlator on the right-hand side. Note that the $+(-)$ external state is associated with the expected $A(\bar{A})$ field only after 'amputating' the corresponding propagator on the right-hand side of (3.1).

A generic correlation function of the A fields may be written schematically in momentum space as

$$\langle \cdots A(p) \cdots \bar{A}(q) \cdots \rangle.$$

However, it is now the B fields which propagate. Therefore, we must regard A and $\bar{A}$ above as functions of B and $\bar{B}$ and make the replacements from the series; again, schematically we can write this as (neglecting the field normalisation factors from (2.25) and (2.26))

$$\left(\cdots \left(\sum_n \Upsilon_{p2\cdots n} B_{\bar{2}} \cdots B_{\bar{n}} \right) \cdots \left(-\sum_{n,s} \frac{\hat{s}}{\hat{q}} \Xi_{q2\cdots n}^{s-1} B_{\bar{2}} \cdots \bar{B}_{\bar{s}} \cdots B_{\bar{n}} \right) \cdots \right). \quad (3.3)$$

Order-by-order, we take Wick contractions between the B field operators with its propagator. This naturally lends itself to a Feynman graph representation where we have vertices for the Υ and Ξ coefficients, the first few of which are shown in figure 2. We refer to these vertices as "MHV completion vertices" and graphs built from them as "MHV completion graphs" since they allow the construction of amplitudes otherwise absent from the theory. (Note that the figure shows the vertices appropriate for $\mathcal{A}$, $\mathcal{B}$, etc. so that the normalisation factors of (2.25) and (2.26) above can be omitted for clarity.)

3.2 Tree-level $(-++)$ amplitude

We obtain the amplitude by amputating the $\langle A\bar{A}\bar{A}\rangle$ correlation function, whose tree-level
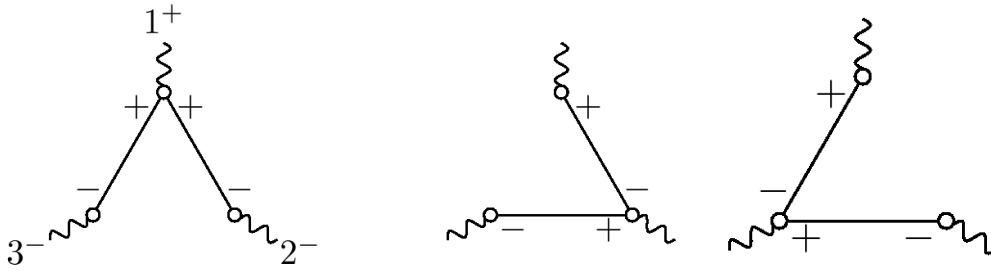
Figure 3: Contributions to the tree-level $(-++)$ amplitude, before applying LSZ reduction.

contributions are shown in figure 3. Hence, we need to take the limit as $p_1^2, p_2^2, p_3^2 \to 0$ of

$$
A(1^-, 2^+, 3^+) = -i p_1^2 p_2^2 p_3^2 \left\{ \frac{1}{p_2^2} \frac{1}{p_3^2} \Upsilon(123) - \frac{1}{p_3^2} \frac{1}{p_1^2} \frac{\hat{1}}{\hat{2}} \Xi^2(231) - \frac{1}{p_1^2} \frac{1}{p_2^2} \frac{\hat{1}}{\hat{3}} \Xi^1(312) \right\} \left(-\frac{ig}{\sqrt{2}} \right)
$$
$$
= \frac{ig}{\sqrt{2}} \frac{\hat{1}^2}{(2\,3)} \left(\frac{p_1^2}{\hat{1}} + \frac{p_2^2}{\hat{2}} + \frac{p_3^2}{\hat{3}} \right)
$$

$$(3.4)$$

In the first line, the leading factor of $-i$ comes from an un-cancelled inverse propagator, and the final factor from the application of (2.25).

The third factor on the second line can further be simplified by applying (A.4), reducing further to

$$
A(1^-, 2^+, 3^+) = ig\sqrt{2} \frac{\hat{1}}{\hat{2}\hat{3}} \{2\,3\}
$$
$$
= ig \frac{[2\,3]^3}{[3\,1][1\,2]},
$$

$$(3.5)$$

the expected $\overline{\text{MHV}}$ amplitude.

As is well known, in order for this to be non-vanishing in the on-shell limit, we need to work with complex momenta or $(2,2)$ signature. However, it is noteworthy that off mass shell it actually coincides with the CSW prescription.

3.3 The origin of equivalence theorem evasion

It may be useful to illustrate the general mechanism behind the S-matrix equivalence theorem [45] with a toy scalar model. We compute correlation functions from the model's partition function by adding a source term $\int d^D x \, j\phi$. Now write the action in terms of a new field variable ϕ' given implicitly by the invertible transformation $\phi = f(\phi', \partial_\mu \phi', \partial_\mu \partial_\nu \phi', \dots)$ where f is a *regular* function of ϕ' and its derivatives. (If it has a non-unit jacobian we can ignore it for the purposes of this discussion.) Upon taking derivatives with respect to j, we see that additional terms of ϕ'^2 and higher powers are also pulled down from the exponential. An insertion of $\phi'^n(x)$ will connect to n propagators, whose momenta sum to that associated with x by the Fourier transform. Unlike when $n = 1$, these propagators do

not, in general, cancel the inverse propagator from LSZ reduction and thus vanish in the on-shell limit. Hence, we can truncate the source term to $\int d^D x\, j\phi'$. At the quantum level, self-energy-like terms can be made from insertions of $\phi'^n(x)$, but this will alter scattering amplitudes by at most a wavefunction renormalisation (as has been discussed in this context in ref. [46]).

The canonical transformation considered here is not local within the quantisation surface but it is local in light-cone time. This vestige of locality is usually sufficient to make the theorem applicable at tree-level because the canonical transformation contains no terms in $\check{p}$ and so cannot produce a factor of $1/p^2$ which contains $\check{p}$ in the denominator. It is therefore remarkable that in certain cases the theorem is circumvented. This can happen when terms collect so that the factor $\sum_j p_j^2/\hat{j}$ is formed, as in (3.4). By (A.5) such terms are independent of $\check{p}$ and can be cancelled by the restricted non-locality introduced through (2.17). As we will see, the same features are responsible for the recovery of the all-+ amplitudes at one loop.

4. The D-dimensional canonical MHV lagrangian

The treatment of quantum corrections to amplitudes in the canonical MHV lagrangian formalism will require that the theory be regulated, and we will do so by dimensional regularisation. It turns out that we can then apply the canonical transformation procedure essentially as before, save for the fact that pieces outside four dimensions result in much richer structure and hence more complicated MHV rules.

4.1 Light-cone Yang-Mills in D dimensions

We write the co-ordinates in $D = 4 - 2\epsilon$ dimensions as:

$$x^0 = \frac{1}{\sqrt{2}}(t - x^{D-1}), \qquad\qquad z^I = \frac{1}{\sqrt{2}}(x^{2I-1} + ix^{2I}),$$
$$x^{\bar{0}} = \frac{1}{\sqrt{2}}(t + x^{D-1}), \qquad\qquad \bar{z}^I = \frac{1}{\sqrt{2}}(x^{2I-1} - ix^{2I}),$$

where the index I runs over the $\frac{1}{2}(2 - 2\epsilon)$ pairs of transverse directions. In these co-ordinates, the metric takes block diagonal form with non-zero components $g_{0\bar{0}} = g_{\bar{0}0} = 1$, $g_{z^I \bar{z}^J} = g_{\bar{z}^I z^J} = -\delta_{IJ}$. Again, we introduce a more compact notation for the components of 1-forms and momenta, for which we write $(p_0, p_{\bar{0}}, p_{z^I}, p_{\bar{z}^J}) \equiv (\check{p}, \hat{p}, p_I, \bar{p}_I)$, with $(\check{n}, \hat{n}, n_I, \bar{n}_I)$ for momenta labelled by a number.

The reason we make this choice of basis is that it will lead us again to a lagrangian with the structure (2.21) and thus inherit some of the simplicity of MHV rules in four space-time dimensions, for example the tree-level properties that the first non-vanishing amplitudes are MHV amplitudes, these coinciding with the lagrangian vertices, that NMHV amplitudes are constructed by joining precisely two such vertices together by the propagator and so on.

In these co-ordinates, the invariant becomes

$$A \cdot B = \check{A}\,\hat{B} + \hat{A}\,\check{B} - A_I \bar{B}_I - \bar{A}_I B_I, \tag{4.1}$$

where we have assumed the summation convention that a repeated capital Roman index in a product is summed over $1, \ldots, 1 - \epsilon$. The bilinears of (2.3) become

$$(1\,2)_I := \hat{1}\hat{2}_I - \hat{2}\hat{1}_I, \quad \{1\,2\}_I := \hat{1}\bar{2}_I - \hat{2}\bar{1}_I. \tag{4.2}$$

They amount to our D dimensional generalisation of the familiar spinor brackets (2.5). Scalar products between these will often be shortened to

$$(1\,2)\cdot\{1\,2\} \equiv (1\,2)_I\{1\,2\}_I,$$

where the dot is obviously redundant when the bilinears are purely four-dimensional.

The Yang-Mills action is written as before in Minkowski co-ordinates as

$$S = \frac{1}{2g^2} \int d^D x \, \text{tr}\mathcal{F}^{\mu\nu}\mathcal{F}_{\mu\nu}. \tag{4.3}$$

The field-strength tensor and group generators are defined as before in (2.7) and (2.8). The quantisation procedure is similar to that in four dimensions. It takes place on surfaces Σ with normal $\mu = (1, 0, \ldots, 0, 1)/\sqrt{2}$ (i.e. of constant x^0) in Minkowski co-ordinates, subject to the axial gauge condition $\mu \cdot \mathcal{A} = \hat{\mathcal{A}} = 0$. We integrate $\check{\mathcal{A}}$ out of the lagrangian and are left with a D-dimensional light-cone action in the form (2.9), where now however

$$L^{-+} = \quad \text{tr} \int_\Sigma d^{D-1}\mathbf{x} \, \mathcal{A}_I(\check{\partial}\hat{\partial} - \partial_J\bar{\partial}_J)\bar{\mathcal{A}}_I, \tag{4.4}$$

$$L^{-++} = -\text{tr} \int_\Sigma d^{D-1}\mathbf{x} \, (\bar{\partial}_I\mathcal{A}_J[\hat{\partial}^{-1}\mathcal{A}_I, \hat{\partial}\bar{\mathcal{A}}_J] + \bar{\partial}_I\bar{\mathcal{A}}_J[\hat{\partial}^{-1}\mathcal{A}_I, \hat{\partial}\mathcal{A}_J]), \tag{4.5}$$

$$L^{--+} = -\text{tr} \int_\Sigma d^{D-1}\mathbf{x} \, (\partial_I\mathcal{A}_J[\hat{\partial}^{-1}\bar{\mathcal{A}}_I, \hat{\partial}\bar{\mathcal{A}}_J] + \partial_I\bar{\mathcal{A}}_J[\hat{\partial}^{-1}\bar{\mathcal{A}}_I, \hat{\partial}\mathcal{A}_J]), \tag{4.6}$$

$$\begin{aligned}
L'^{--++} = -\text{tr} \int_\Sigma d^{D-1}\mathbf{x} \, \Big(&\frac{1}{4}[\hat{\partial}\mathcal{A}_I, \bar{\mathcal{A}}_I]\,\hat{\partial}^{-2}\,[\hat{\partial}\mathcal{A}_J, \bar{\mathcal{A}}_J] \\
&+ \frac{1}{2}[\hat{\partial}\mathcal{A}_I, \bar{\mathcal{A}}_I]\,\hat{\partial}^{-2}\,[\hat{\partial}\bar{\mathcal{A}}_J, \mathcal{A}_J] \\
&- \frac{1}{4}[\hat{\partial}\bar{\mathcal{A}}_I, \mathcal{A}_I]\,\hat{\partial}^{-2}\,[\hat{\partial}\bar{\mathcal{A}}_J, \mathcal{A}_J] \\
&- \frac{1}{4}[\mathcal{A}_I, \mathcal{A}_J][\bar{\mathcal{A}}_I, \bar{\mathcal{A}}_J] - \frac{1}{4}[\mathcal{A}_I, \bar{\mathcal{A}}_J][\bar{\mathcal{A}}_I, \mathcal{A}_J]\Big).
\end{aligned} \tag{4.7}$$

It may be shown with integration by parts that these expressions reduce in four dimensions to those of section 2.2.

4.2 The transformation

We will now specify the change of field variables from $\mathcal{A}$ and $\bar{\mathcal{A}}$ to $\mathcal{B}$ and $\bar{\mathcal{B}}$. From (4.4), we see that the momentum conjugate to $\mathcal{A}_I$ is $\Pi_I(x) = -\hat{\partial}\bar{\mathcal{A}}_I(x)$, and as such

$$\mathcal{D}\mathcal{A}\,\mathcal{D}\Pi \equiv \prod_{x,I} d\mathcal{A}_I(x)\,d\Pi_I(x) \tag{4.8}$$

is proportional (up to a constant) to the path integral measure $\mathcal{D}\mathcal{A}\mathcal{D}\bar{\mathcal{A}}$; therefore a canonical field transformation will have unit jacobian. We can implement this by requiring that $\mathcal{A}$ be a functional of $\mathcal{B}$ alone, subject to either of the following equivalent conditions:

$$\hat{\partial}\bar{\mathcal{A}}_I^a(x^0, \mathbf{x}) = \int_\Sigma d^{D-1}\mathbf{y}\, \frac{\delta\mathcal{B}_J^b(x^0, \mathbf{y})}{\delta\mathcal{A}_I^a(x^0, \mathbf{x})} \hat{\partial}\bar{\mathcal{B}}_J^b(x^0, \mathbf{y}), \tag{4.9}$$

$$\mathrm{tr}\int_\Sigma d^{D-1}\mathbf{x}\, \check{\partial}\mathcal{A}_I\, \hat{\partial}\bar{\mathcal{A}}_I = \mathrm{tr}\int_\Sigma d^{D-1}\mathbf{x}\, \check{\partial}\mathcal{B}_I\, \hat{\partial}\bar{\mathcal{B}}_I. \tag{4.10}$$

Again, working in momentum space on the quantisation surface, we express $\mathcal{A}$ as a series in $\mathcal{B}$, but this time the series coefficients carry extra indices for the transverse directions:

$$\mathcal{A}_{I_1}(\mathbf{p}_1) = \sum_{n=2}^\infty \int_{2\cdots n} \Upsilon_{I_1\cdots I_n}(1\cdots n)\, \mathcal{B}_{I_2}(-\mathbf{p}_2)\cdots\mathcal{B}_{I_n}(-\mathbf{p}_n) \tag{4.11}$$

where $\Upsilon_{IJ}(12) = \delta(\mathbf{p}_1 + \mathbf{p}_2)\delta_{IJ}$. The integral short-hand here is defined by

$$\int_{1\cdots n} = \prod_{k=1}^n \frac{1}{(2\pi)^{3-2\epsilon}} \int d\hat{k} \prod_{I=1}^{1-\epsilon} dk_I d\bar{k}_I$$

and for later use we introduce the δ-function stripped form of a coefficient, given (as the first factor on the right-hand side) by

$$\Upsilon_{I_1\cdots I_n}(1\cdots n) = \Upsilon(1^{I_1}\cdots n^{I_n})\,(2\pi)^{3-2\epsilon}\delta(\mathbf{p}_1 + \cdots + \mathbf{p}_n) \tag{4.12}$$

and similarly for the other vertices Ξ, V and W, defined below. They should only be considered to be defined when the sum of their momentum arguments is 0. Repeated transverse indices in the superscripts are also subject to the summation convention. For convenience, we will often also subsume the index into the momentum label when the association is obvious (e.g. $\Upsilon(1^{I_1}\cdots n^{I_n}) \to \Upsilon(1\cdots n)$ above).

The canonical transformation removes the $(-++)$ terms from the lagrangian by absorbing them into the kinetic term for $\mathcal{B}$:

$$L^{-+}[\mathcal{A}] + L^{-++}[\mathcal{A}] = L^{-+}[\mathcal{B}]. \tag{4.13}$$

Briefly delving into momentum space on the quantisation surface, it is seen that the term on the right-hand side of (4.13) furnishes the tree-level propagator

$$\langle\mathcal{B}_I\bar{\mathcal{B}}_J\rangle = -\frac{ig^2}{2p^2}\delta_{IJ}. \tag{4.14}$$

Similarly, from the quantisation surface Fourier transform of (4.5), expanding the commutator and re-labelling leads us to

$$L^{-++} = \mathrm{tr}\int_{123} \bar{V}_{IJK}^2(123)\, \mathcal{A}_I(\bar{1})\mathcal{A}_J(\bar{2})\bar{\mathcal{A}}_K(\bar{3}) \tag{4.15}$$

where

$$\bar{V}^2(1^I 2^J 3^K) = i\left(\frac{\{3\,1\}_J \delta_{KI}}{\hat{2}} + \frac{\{2\,3\}_I \delta_{JK}}{\hat{1}}\right). \tag{4.16}$$

It obviously follows from (4.13) and the light-cone lagrangian that this is the D dimensional equivalent of the $(++-)$ $\overline{\text{MHV}}$ vertex for the $\mathcal{A}$ field, and this is reflected in our choice of notation.

The remaining pieces of the lagrangian, (4.6) and (4.7), form MHV vertices in $4 - 2\epsilon$ dimensions, as explained in the next section. To obtain the Υ coefficients, we take the explicit expression of (4.13) and use (4.9) and (4.10) to further reduce it to

$$\left\{ \frac{\partial \cdot \bar{\partial}}{\hat{\partial}} \mathcal{A}_I - [\bar{\partial}_J \mathcal{A}_I, \hat{\partial}^{-1} \mathcal{A}_J] - \frac{\bar{\partial}_J}{\hat{\partial}} [\hat{\partial}^{-1} \mathcal{A}_J, \partial \mathcal{A}_I] \right\}(\mathbf{x}) = \int_\Sigma d^3 \mathbf{y} \, \frac{\delta \mathcal{A}_I(\mathbf{x})}{\delta \mathcal{B}_J^b(\mathbf{y})} \left(\frac{\partial \cdot \bar{\partial}}{\hat{\partial}} \right)_{\mathbf{y}} \mathcal{B}_J^b(\mathbf{y}). \tag{4.17}$$

By again transforming to momentum space and substituting the series expansion for $\mathcal{A}$ into both sides of (4.17) above, carefully rearranging the fields, and comparing terms order-by-order in $\mathcal{B}$, we extract successive Υ coefficients. At $\mathcal{O}(\mathcal{B}^2)$, one finds

$$\Upsilon(1^I 2^J 3^K) = \frac{i}{(2\,3) \cdot \{2\,3\}} (\hat{2} \{2\,3\}_K \delta_{IJ} + \hat{3} \{2\,3\}_J \delta_{KI}) \tag{4.18}$$

$$= -\frac{1}{\hat{1}} \frac{\bar{V}^2(2^J 3^K 1^I)}{(\Omega_1 + \Omega_2 + \Omega_3)}$$

$$= \frac{2}{\hat{1}} \frac{\bar{V}^2(2^J 3^K 1^I)}{p_1^2/\hat{1} + p_2^2/\hat{2} + p_3^2/\hat{3}} \tag{4.19}$$

and for compactness we have defined

$$\Omega_p := \frac{p_I \bar{p}_I}{\hat{p}}.$$

By continuation of this process, we arrive at the following recursion relation for Υ:

$$\Upsilon(1 \cdots n) = -\frac{i}{\sum_{i=1}^n \Omega_i} \sum_{j=2}^{n-1} [\zeta(1, P_{j+1,n}^B, P_{2j}^A) - \zeta(1, P_{2j}^A, P_{j+1,n}^B)] \tag{4.20}$$
$$\times \Upsilon(-^A, 2, \ldots, j) \Upsilon(-^B, j+1, \ldots, n),$$

where $P_{ij} := p_i + p_{i+1} \cdots + p_j$ and we have introduced the symbol

$$\zeta(1^I 2^J 3^K) := \frac{\{2\,3\}_K \delta_{IJ}}{\hat{3}(\hat{2} + \hat{3})}.$$

An alternative form for this expression follows from (4.13):

$$\Upsilon(1 \cdots n) = -\frac{1}{\hat{1} \sum_{i=1}^n \Omega_i} \sum_{j=2}^{n-1} \bar{V}^2(P_{2j}^A, P_{j+1,n}^B, 1) \Upsilon(-^A, 2, \ldots, j) \Upsilon(-^B, j+1, \ldots, n), \tag{4.21}$$

Of course it is no accident that the recurrence relation and its solutions can be expressed in terms of $\bar{V}^2$ in this way. The canonical transformation that absorbs this interaction into the kinetic term in (4.13) can be performed for any choice of $\bar{V}^2$. This will be important later on, since it clarifies how the amplitudes involving the missing $\bar{V}^2$ vertex are recovered, and also demonstrates that the mechanism of recovery is generic in any theory where a

canonical transformation is used to absorb a three point vertex into the kinetic term as in (4.13).

A useful particular case of this formula is

$$\Upsilon(1234) = \frac{1}{\hat{1}\sum_{i=1}^{4}\Omega_i}\left\{\bar{V}^2(2,\bar{5}^A,1)\frac{1}{\hat{5}(\Omega_5+\Omega_3+\Omega_4)}\bar{V}^2(3,4,5^A)\right.$$
$$\left.+\,\bar{V}^2(\bar{5}^A,4,1)\frac{1}{\hat{5}(\Omega_5+\Omega_2+\Omega_3)}\bar{V}^2(2,3,5^A)\right\}. \tag{4.22}$$

Note that here (and throughout) 5 is a dummy momentum with scope limited to each term, and that its value should be taken to be the negative of the sum of the other arguments that accompany it a vertex.

Differentiating (4.11) with respect to $\mathcal{B}$ and inserting the inverse into (4.9) suggests a series expansion for $\bar{\mathcal{A}}$ of the form

$$\bar{\mathcal{A}}_{I_1}(-\mathbf{p}_1) = \sum_{n=2}^{\infty}\sum_{s=2}^{n}\int_{2\cdots n}\frac{\hat{s}}{\hat{1}}\Xi^{s-1}_{I_1\cdots I_n}(\bar{1}2\cdots n)\,\mathcal{B}_{I_2}(-\mathbf{p}_2)\cdots\bar{\mathcal{B}}_{I_s}(-\mathbf{p}_s)\cdots\mathcal{B}_{I_n}(-\mathbf{p}_n). \tag{4.23}$$

Now, inserting (4.11) and (4.23) into (4.10), and then comparing coefficients order-by-order in $\mathcal{B}$, we may obtain expressions for the Ξ coefficients in terms of other Ξs and Υs of lower order. The results

$$\Xi^1(1^I2^J3^K) = -\Upsilon(2^J3^K1^I) \quad\text{and}\quad \Xi^2(1^I2^J3^K) = -\Upsilon(3^K1^I2^J) \tag{4.24}$$

will be of particular relevance to the forthcoming. By careful examination of the expansion of (4.10) at the $(n-1)^{\text{th}}$ order in $\mathcal{B}$, one finds that this recursion relation

$$\Xi^s(1\cdots n) = -\sum_{r=\max(2,4-s)}^{n+1-s}\sum_{m=\max(r,3)}^{r+s-1}\Upsilon(-^A,3-r,\ldots,m+1-r)$$
$$\times\,\Xi^{r+s-m}(-^A,m+2-r,\ldots,2-r). \tag{4.25}$$

holds, given that $\Xi(1^I2^J) = \delta_{IJ}$.

As in section 3.1, we introduce a diagrammatic representation of Υ and Ξ in the form of D-dimensional MHV completion vertices, the first few of which are shown in figure 4. We note that the process of deriving Υ and Ξ in $4-2\epsilon$ dimensions differs only from that in four dimensions by the presence of extra transverse indices, which are seen to each ride alongside (and can therefore be built into) a momentum index. It is therefore not surprising that the relationship between Υ and Ξ is, from this point of view, identical to that in four dimensions.

4.3 The hyper-MHV rules

We will now extract the $4-2\epsilon$-dimensional generalisations of the three and four gluon MHV amplitudes. The interaction part of the lagrangian takes the same form as (2.22) except that the vertices carry polarisation indices to contract into the corresponding $\mathcal{B}$s
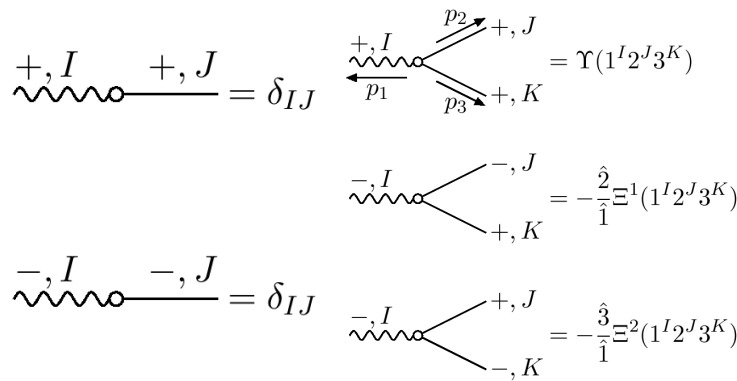
Figure 4: D-dimensional Υ and Ξ MHV completion vertices.

and $\bar{\mathcal{B}}$s. The Feynman rule for a particular $\mathcal{B}$ vertex is thus $4iV^s(1^{I_1} \cdots n^{I_n})/g^2$, and this follows from the definition as the sum of all contractions of external lines into the term in the action with the matching colour factor, while accounting for the cyclic symmetry of the trace.

The three-point MHV vertex can be obtain in a manner almost identical to how (4.16) was derived. In quantisation surface momentum-space, (4.6) reads

$$L^{--+} = \text{tr} \int_{123} V_{IJK}^2(123) \, \bar{\mathcal{A}}_I(\bar{1})\bar{\mathcal{A}}_J(\bar{2})\mathcal{A}_K(\bar{3}) \tag{4.26}$$

where

$$V^2(1^I 2^J 3^K) = i\left(\frac{(3\,1)_J \delta_{KI}}{\hat{2}} + \frac{(2\,3)_I \delta_{JK}}{\hat{1}} \right). \tag{4.27}$$

Since $\mathcal{A} = \mathcal{B}$ and $\bar{\mathcal{A}} = \bar{\mathcal{B}}$ to leading order, upon substituting (4.11) and (4.23) into (4.26), we immediately see that $V^2(1^I 2^J 3^K)$ is the $\bar{\mathcal{B}}_I(1)\bar{\mathcal{B}}_J(2)\mathcal{B}_K(3)$ colour-ordered vertex.

We note that $\bar{\mathcal{B}}\bar{\mathcal{B}}\mathcal{B}\mathcal{B}$ and $\bar{\mathcal{B}}\mathcal{B}\bar{\mathcal{B}}\mathcal{B}$ colour-ordered vertices receive contributions from $L^{--+}[\mathcal{A}]$ and $L'^{--++}[\mathcal{A}]$. Upon writing the latter in momentum-space, we have

$$L'^{--++} = \text{tr} \int_{1234} \left\{ W_{IJKL}^2(1234) \, \bar{\mathcal{A}}_I(\bar{1})\bar{\mathcal{A}}_J(\bar{2})\mathcal{A}_K(\bar{3})\mathcal{A}_L(\bar{4}) \right. \tag{4.28}$$
$$\left. + W_{IJKL}^3(1234) \, \bar{\mathcal{A}}_I(\bar{1})\mathcal{A}_J(\bar{2})\bar{\mathcal{A}}_K(\bar{3})\mathcal{A}_L(\bar{4}) \right\}$$

where

$$W^2(1^I 2^J 3^K 4^L) = \delta_{IK}\delta_{JL} + \delta_{IL}\delta_{JK}\frac{\hat{1}\hat{2} + \hat{3}\hat{4}}{(\hat{1} + \hat{4})^2}, \tag{4.29}$$

$$W^3(1^I 2^J 3^K 4^L) = \frac{1}{2}\left(\delta_{IL}\delta_{JK}\frac{\hat{1}\hat{2} + \hat{3}\hat{4}}{(\hat{1} + \hat{4})^2} + \delta_{IJ}\delta_{KL}\frac{\hat{1}\hat{4} + \hat{2}\hat{3}}{(\hat{1} + \hat{2})^2} \right). \tag{4.30}$$

We substitute (4.11) and (4.23) into $L^{--+}[\mathcal{A}] + L'^{--++}[\mathcal{A}]$, and collect the terms of each colour (trace) order of $\mathcal{O}(\mathcal{B}^4)$. Contracting external lines in a colour-ordered manner into

these terms, we have

$$V^2(1234) = \frac{\hat{1}}{5}V^2(5^A23)\Xi^2(\bar{5}^A41) + \frac{\hat{2}}{5}V^2(15^A4)\Xi^1(\bar{5}^A23)$$
$$+ V^2(125^A)\Upsilon(\bar{5}^A34) + W^2(1234) \tag{4.31}$$

for the $\bar{\mathcal{B}}_I(1)\bar{\mathcal{B}}_J(2)\mathcal{B}_K(3)\mathcal{B}_L(4)$ vertex, and

$$V^3(1234) = \frac{\hat{1}}{5}V^2(5^A34)\Xi^1(\bar{5}^A12) + \frac{\hat{3}}{5}V^2(15^A4)\Xi^2(\bar{5}^A23)$$
$$+ \frac{\hat{3}}{5}V^2(5^A12)\Xi^2(\bar{5}^A34) + \frac{\hat{1}}{5}V^2(35^A2)\Xi^1(\bar{5}^A41) \tag{4.32}$$
$$+ 2W^3(1234)$$

for the $\bar{\mathcal{B}}_I(1)\mathcal{B}_J(2)\bar{\mathcal{B}}_K(3)\mathcal{B}_L(4)$ vertex.

That these expressions reduce in four dimensions should be obvious by comparing the forms of (4.31) and (4.32) to their four-dimensional analogs in ref. [46] and noting the reduction of the individual factors.
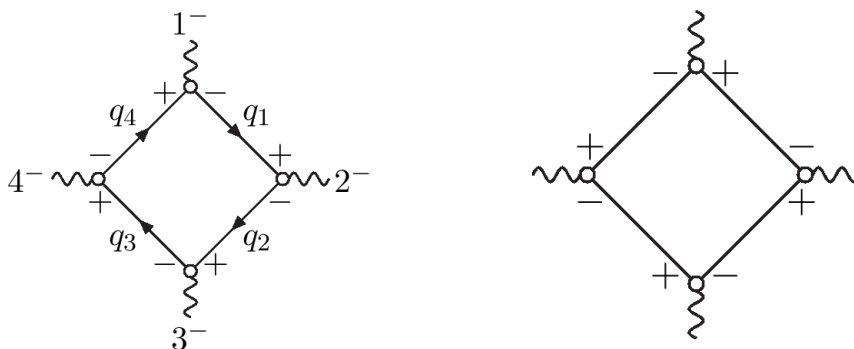
5. The one-loop $(++++)$ amplitude

It is not possible to construct a one-loop $(++++)$ amplitude using only the $\mathcal{B}$ vertices of the canonical MHV lagrangian. Nevertheless, we know it is non-vanishing (see, e.g., [57, 58, 17, 16, 59]). We will see that it arises (as it indeed must) from equivalence theorem evading pieces, constructed from the MHV completion vertices of figure 4.

In all, we can construct four classes of graphs for this contribution: boxes, triangles, two classes of bubbles (corresponding to the two possible arrangements of external lines on either side of the loop), and the tadpoles.

In the next three subsections, we will consider the generalised quadruple cut of these diagrams. We will restrict ourselves to analysing the cuts that arise from the singularities provided by the propagators, which we refer to as *standard* cuts. From general considerations [54] we expect other *non-standard* cuts arising from the singular denominators in the vertices. This is true both of the D dimensional version we have here and the four dimensional Parke-Taylor forms (2.27). From the earlier derivation it is clear that this singular behaviour is restricted to the quantisation surface (they have no dependence on $\breve{p}$). These cuts therefore depend on the orientation of the quantisation surface, i.e. μ, and are thus gauge artifacts which should all cancel out in any complete on-shell amplitude.

In general, by the Feynman tree theorem [31, 55], we can reconstruct the amplitude entirely using only the standard cuts since only these involve a change in light cone time. However, we will not follow this procedure here since we will be content to show instead in the last two subsections that the diagrams we construct simply sum up to the contributions one would have obtained from the original light cone Yang-Mills lagrangian (2.9) (even before integration over the loop momentum).

Figure 5: Box contributions to the one-loop $(++++)$ amplitude. All external momenta are taken as outgoing.

5.1 Off-shell quadruple cut

First, consider the contribution to the standard quadruple cut coming from the box diagram, shown in figure 5. The amplitude is obtained by amputating $\langle \bar{A}\bar{A}\bar{A}\bar{A}\rangle$, the box diagram for which is shown in figure 5. This gives a contribution of

$$
A^{\mathrm{box}}(1^+, 2^+, 3^+, 4^+) = \lim_{p_1^2, p_2^2, p_3^2, p_4^2 \to 0} \frac{1}{4} g^4 \frac{p_1^2 p_2^2 p_3^2 p_4^2}{\hat{1}\hat{2}\hat{3}\hat{4}} \int \frac{d^D q}{(2\pi)^D} \frac{16}{q_1^2 q_2^2 q_3^2 q_4^2} \frac{1}{\Sigma_1 \Sigma_2 \Sigma_3 \Sigma_4} \times
$$
$$
\left\{ \bar{V}^2(-q_4^D, 1, q_1^A) \bar{V}^2(-q_1^A, 2, q_2^B) \bar{V}^2(-q_2^B, 3, q_3^C) \bar{V}^2(-q_3^C, 4, q_4^D) \right.
$$
$$
\left. + \bar{V}^2(1, q_1^A, -q_4^D) \bar{V}^2(2, q_2^B, -q_1^A) \bar{V}^2(3, q_3^C, -q_2^B) \bar{V}^2(4, q_4^D, -q_3^C) \right\},
$$
(5.1)

where we have already used (4.24), the internal momenta are defined as $q_i = q - P_{1i}$, and we define the short-hand

$$
\Sigma_j := \frac{q_j^2}{\hat{q}_j} - \frac{q_{j-1}^2}{\hat{q}_{j-1}} + \frac{p_j^2}{\hat{p}_j}
$$
(5.2)

(indices interpreted cyclically). Note that the external momenta $p_1, \ldots, p_4$ are in four dimensions and thus their transverse indices have all been set to one.

Before going on to compute the quadruple standard cut of the box, as an aside we will show that its double and triple standard cuts vanish for on-shell external momenta. Consider cutting any three internal lines of figure 5, where by this we mean strictly to analyse only those parts of phase space where the remaining internal line stays off-shell. Without loss of generality, we choose these internal lines to be q_1, q_2 and q_3. In order that the amplitude survives LSZ reduction, the correlator must generate a singularity in $p_1^2 p_2^2 p_3^2 p_4^2$. Clearly, the Σ_2 and Σ_3 denominators provide a singularity $p_2^2 p_3^2$ once the internal lines are cut. We now claim that the triple cut vanishes as follows: the required singularity in $p_1^2 p_4^2$ must come from the denominators in the remaining tree graph connecting p_1 and p_4. The relevant factors from (5.1) are the q_4 propagator, and the Σ_1 and Σ_4 denominators,

i.e.

$$\frac{1}{q_4^2} \left(\frac{q_1^2}{\hat{q}_1} - \frac{q_4^2}{\hat{q}_4} + \frac{p_1^2}{\hat{p}_1} \right)^{-1} \left(\frac{q_4^2}{\hat{q}_4} - \frac{q_3^2}{\hat{q}_3} + \frac{p_4^2}{\hat{p}_4} \right)^{-1}.$$

Upon setting q_1^2 and q_3^2 to zero and discarding (the non-vanishing) factors of momenta that appear on the numerator, we arrive at

$$\frac{1}{q_4^2} \frac{1}{\hat{q}_4 \, p_1^2 - \hat{1} \, q_4^2} \frac{1}{\hat{4} \, q_4^2 + \hat{q}_4 \, p_4^2}.$$

The above factors clearly cannot cancel $p_1^2 p_4^2$ so long as $q_4^2 \neq 0$. Hence this cut vanishes as we take all the external momenta on shell. By similar consideration, one can also see that both possible double cuts of this graph also vanish.

Now, we will compute the standard quadruple cut. This is obtained by putting all four internal lines on shell [54, 34, 23]. The external momenta are kept off shell momentarily. We see that the Σ_i reduce to $p_i^2/\hat{i}$ factors upon cutting, producing poles which thus cancel the factors of p_i^2 from LSZ reduction and the $1/\hat{i}$ factors. The remaining terms have a finite non-vanishing[2] on-shell limit and it is already clear that they are exactly what we obtain from the four-cut box contribution using the light cone Yang-Mills lagrangian (2.9).

For the purposes of demonstrating that precisely this contribution arises from the four-cut MHV completion box graph within the present formalism we do not need to go any further. However, let us show how this contribution can be straightforwardly computed within the bracket formalism we have developed here and in ref. [46].

5.2 Explicit evaluation

First note that the external momenta remain four-dimensional, whereas the loop momentum $q \equiv q_4$ in the integral is D-dimensional. The solution to the four constraints $q_i^2 = 0$ fixes the four-dimensional part of q to a discrete set of solutions (in fact two); these are functions of the remaining, orthogonal -2ϵ components μ. Now since q can only contract with either itself or the four-dimensional external momenta, we see that these solutions can in fact only depend on $\mu^2 = 2(q_I \bar{q}_I - \tilde{q}\bar{q})$.

All external momenta are now on shell in the forthcoming analysis. Substituting for the vertices, we find the remaining cut integral to be

$$8g^4(1-\epsilon) \frac{1}{\hat{1}\hat{2}\hat{3}\hat{4}} \int \frac{d\mu^{-2\epsilon}}{(2\pi)^{-2\epsilon}} \{q\,1\}\{q-1,2\}\{q+4,3\}\{q\,4\}, \tag{5.3}$$

where we have split the integral over momentum space as in [59]. Note that the $\{\cdots\}$ bilinears above have their index set to 1, but this has been dropped for clarity.

We also remind the reader that the four dimensional part of q is now a function of μ^2, and note that the factor of $(1-\epsilon)$ comes from dimensional regularisation of the gauge field degrees of freedom (as opposed to 'dimensional reduction', which only extends the loop momentum to D dimensions and therefore lacks this factor). In the following, since

---

[2]Recall that four-cut solutions are non-vanishing because they use complex external and internal momenta [54, 34, 23].

the momenta are complex, $\{q\,1\}$ is not related by complex conjugation to $(q\,1)$. We also remind the reader that the four dimensional part Solutions for the bilinears in (5.3) are evaluated directly. First, consider $(q\,1)\cdot\{q\,1\}$. Since, $q_1^2 = q^2 = p_1^2 = 0$, (A.2), or (A.4), implies that this vanishes. Splitting away the four-dimensional part gives

$$(q\,1)\{q\,1\} + \hat{1}^2\mu^2/2 = 0, \tag{5.4}$$

and similarly

$$(q{-}1,2)\{q{-}1,2\} + \hat{2}^2\mu^2/2 = 0 \quad \text{and} \tag{5.5}$$
$$(q\,4)\{q\,4\} + \hat{4}^2\mu^2/2 = 0. \tag{5.6}$$

We eliminate μ^2 between (5.4), (5.5) and (5.6), and then use (A.3) to eliminate $(q\,4)$ and its conjugate to obtain a quadratic equation

$$\alpha(q\,1)^2 + \hat{1}(q\,1) - \bar{\alpha}\frac{\hat{1}^2\mu^2}{2} = 0 \tag{5.7}$$

where[3]

$$\alpha = \frac{\hat{4}}{(1\,4)} - \frac{\hat{2}}{(1\,2)}, \quad \bar{\alpha} = \frac{\hat{4}}{\{1\,4\}} - \frac{\hat{2}}{\{1\,2\}}. \tag{5.8}$$

This has solutions

$$(q\,1) = -\frac{\hat{1}}{2\alpha}(1\pm\beta), \quad \{q\,1\} = -\frac{\hat{1}}{2\bar{\alpha}}(1\mp\beta), \quad \beta = \sqrt{1 + 2\alpha\bar{\alpha}\mu^2}. \tag{5.9}$$

Next, the Bianchi-like identity (A.3) gives

$$\hat{1}\{q{-}1,2\} = \hat{2}\{q\,1\} + (\hat{q} - \hat{1})\{1\,2\}. \tag{5.10}$$

We apply this equation, its conjugate, and (5.4) to (5.5) to obtain an expression for $\hat{q} - \hat{1}$ in terms of $(q\,1)$ and $\{q\,1\}$. Inserting this back into (5.10) and using (5.9) gives

$$\{q{-}1,2\} = \frac{\hat{2}}{2\alpha}\frac{\{1\,2\}}{(1\,2)}(1\pm\beta). \tag{5.11}$$
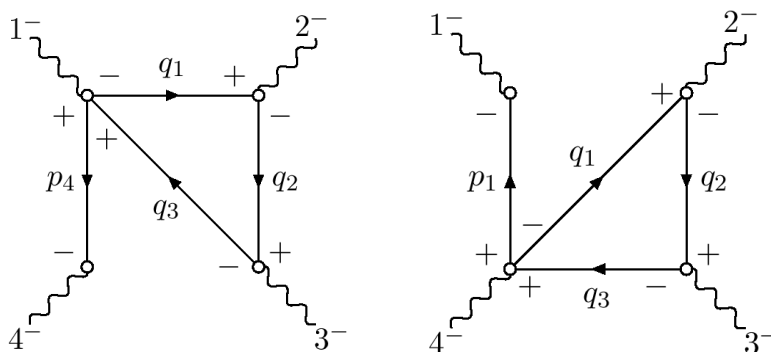
Similarly, we find

$$\{q\,4\} = \frac{\hat{4}}{2\alpha}\frac{\{1\,4\}}{(1\,4)}(1\pm\beta). \tag{5.12}$$

To obtain the final bilinear, we use (A.3) twice to obtain $\{q{+}4,3\}$ in terms of $\{q\,1\}$ and $\{q\,4\}$. (A.4) is then applied to eliminate a quotient of $(\cdots)$ bilinears present in one of the terms in favour of conjugate bilinears, giving

$$\{q{+}4,3\} = \frac{1}{2}\frac{\{2\,3\}\{3\,4\}}{\{2\,4\}}(1\pm\beta). \tag{5.13}$$

---

[3]Again, note that here $\bar{\alpha} \neq \alpha^*$.

Figure 6: One-loop MHV completion triangle graphs for the $(++++)$ amplitude. Note that the propagator carrying an external momentum is attached to the Ξ vertex differently in each case.

Assembling the product of the $\{\cdots\}$ bilinears from (5.9), (5.11), (5.12) and (5.13), we have

$$\{q\,1\}\{q-1,2\}\{q+4,3\}\{q\,4\} = -\frac{1}{4}\hat{1}^2\hat{2}\hat{4}\,\mu^4\,\frac{\{2\,3\}\{3\,4\}}{(1\,2)(4\,1)} = -\frac{1}{4}\hat{1}\hat{2}\hat{3}\hat{4}\,\mu^4\,\frac{\{1\,2\}\{3\,4\}}{(1\,2)(3\,4)} \quad (5.14)$$

for either of the solutions (5.9), where in the second assertion we have used the fact that the right-hand side of (A.4) is zero for null p_j. Using this in (5.3) and reinstating the propagators, we arrive at

$$2(1-\epsilon)g^4\frac{\{1\,2\}\{3\,4\}}{(1\,2)(3\,4)}\int\frac{d^4q\,d^{-2\epsilon}\mu}{(2\pi)^D}\frac{\mu^4}{q_1^2q_2^2q_3^2q_4^2} \quad (5.15)$$

from which one observes that (5.1) has precisely the quadruple cut of the $4-2\epsilon$-dimensional box function K_4, as expected of this amplitude [57, 58, 17, 16, 59].

5.3 Triangle, bubble and tadpole contributions

Typical triangle, bubble and tadpole contributions to the one-loop $(++++)$ amplitude with internal helicities running from $-$ to $+$ in a clockwise sense[4] are shown in figures 6, 7 and 8.

Despite appearances, these diagrams do have quadruple cuts as a result of the singularities in the vertices. We therefore have to consider also cutting the vertices. Let us first consider the quadruple cut of the triangle graph. We can restrict our analysis to the graphs figure 6. Their contribution to the $(++++)$ amplitude is

$$\lim_{p_1^2,p_2^2,p_3^2,p_4^2\to0}\frac{1}{4}g^4\,\frac{p_1^2p_2^2p_3^2p_4^2}{\hat{1}\hat{2}\hat{3}\hat{4}}\int\frac{d^Dq}{(2\pi)^D}\frac{\hat{q}_1\hat{q}_2\hat{q}_3}{q_1^2q_2^2q_3^2}\times$$

$$\left\{-\Xi^1(1,q_1^A,-q_3^C,4)\Xi^1(2,q_2^B,-q_1^A)\Xi^1(3,q_3^C,-q_2^B)\frac{\hat{4}}{p_4^2}\right. \quad (5.16)$$

$$\left.-\Xi^2(4,1,q_1^A,-q_3^C)\Xi^2(2,q_2^B,-q_1^A)\Xi^2(3,q_3^C,-q_2^B)\frac{\hat{1}}{p_1^2}\right\}.$$

---

[4]The "sense" of internal helicity orientation is always defined in this paper as propagating from $-$ to $+$.
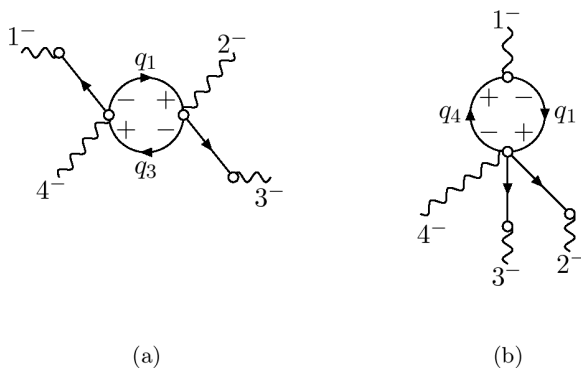
Figure 7: MHV completion bubble graphs. In (a) we show a the 2|2 bubble. There are three other graphs like it (up to shifting the external momentum labels once by $i \to i+1$) obtained by swapping the external momentum propagators between gluons 1 and 4, and between gluons 2 with 3. The 3|1 bubble is shown in (b); there are two additional graphs (up to rotations of the labels), in this case obtained by associating the wavy line attached to the five-point Ξ with gluon 2 or 3 instead of 4.
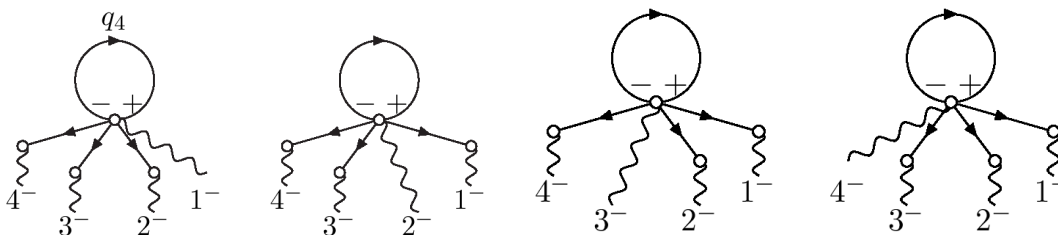
Figure 8: Tadpole MHV completion graphs. Notice that the coupling of the six-point Ξ to the $\bar{A}$ field (denoted by the wavy line) is associated with a different gluon in each case.

Using the recursion relations (4.20) and (4.25), we can re-write this as

$$
\lim_{p_1^2,p_2^2,p_3^2,p_4^2 \to 0} \frac{1}{4} g^4 \frac{p_1^2 p_2^2 p_3^2 p_4^2}{\hat{1}\hat{2}\hat{3}\hat{4}} \int \frac{d^D q}{(2\pi)^D} \frac{16}{q_1^2 q_2^2 q_3^2} \left\{ \frac{X}{\hat{q}_4 \Sigma_1 \Sigma_2 \Sigma_3 \Sigma_4 (\Sigma_1 + \Sigma_4)} \left(\frac{\Sigma_1 \hat{4}}{p_4^2} - \frac{\Sigma_4 \hat{1}}{p_1^2} \right) \right.
$$
$$
\left. + \frac{Y}{(\hat{1} + \hat{4}) \Sigma'_{1+4} \Sigma_2 \Sigma_3} \left(\frac{1}{\Sigma_{1+4}} - \frac{1}{\Sigma_1 + \Sigma_4} \right) \left(\frac{\hat{1}}{p_1^2} + \frac{\hat{4}}{p_4^2} \right) \right\} \tag{5.17}
$$

with

$$
X = \bar{V}^2(-q_4^D, 1, q_1^A) \bar{V}^2(-q_1^A, 2, q_2^B) \bar{V}^2(-q_2^B, 3, q_3^C) \bar{V}^2(-q_3^C, 4, q_4^D), \tag{5.18}
$$
$$
Y = \bar{V}^2(4, 1, 2 + 3^D) \bar{V}^2(-q_3^C, 1 + 4^D, q_1^A) \bar{V}^2(-q_1^A, 2, q_2^B) \bar{V}^2(-q_2^B, 3, q_3^C), \tag{5.19}
$$

$q_4 := q_3 - p_4$ flowing "through" the vertex attached to p_1 (or p_4) as part of a box-like momentum-flow topology (see section 5.4 below for a further investigation of this), and we

define the following extensions of Σ_i as

$$\Sigma_{1+4} := \frac{q_1^2}{\hat{q}_1} - \frac{q_3^2}{\hat{q}_3} + \frac{(p_1 + p_4)^2}{\hat{1} + \hat{4}}, \tag{5.20}$$

$$\Sigma'_{1+4} := \frac{p_1^2}{\hat{1}} + \frac{p_4^2}{\hat{4}} - \frac{(p_1 + p_4)^2}{\hat{1} + \hat{4}}. \tag{5.21}$$

Note that one can write down expressions for the analogues of X and Y from graphs with internal helicities of an anti-clockwise sense. The reader may check for the case at hand (where $\bar{V}^2$ is the three-point $\overline{\text{MHV}}$ vertex), that these are the same as in the clockwise scenario.

Now, recall that we are only studying the standard cuts. We will extract such a quadruple cut contribution here, by keeping the external momenta off the mass shell, and look for any terms containing $1/q_4^2$ in addition to the three propagators already appearing in (5.17). Clearly, by inspection of the Σ_i factors in (5.17), no such $1/q_4^2$ are generated. Indeed it is impossible to generate such terms from the vertices since the singularity in $1/q_4^2$ is not restricted to the quantisation surface. Although the inverse Σ_is and Σ_{1+4} appear in (5.2) and above to yield singularities that look superficially similar to those from propagators, by (A.5) these terms do not contain $\check{q}$ components and thus their singularities lie entirely within the quantisation surface.

A similar analysis of the graphs of figures 7 and 8 leads one quickly to the same conclusion: they have no contribution to the quadruple cut for off-shell external momenta, because in this region none of the denominators from their Ξ vertices form the necessary propagators.[5] Hence, we see that for the one-loop $(++++)$ amplitude in the canonical MHV lagrangian formalism, if we keep the external momenta off shell until after the cuts, only the box graph of figure 5 contributes to the quadruple cut.

5.4 Light-cone Yang-Mills reconstructions

The expressions (5.1), (5.18) and (5.19) begin to elucidate the underlying relationship between the MHV completion graphs of figures 5–8 and the Feynman graphs one would use to compute the same amplitude in conventional perturbative LCYM. We already see parallels of the latter in the topology of the linking amongst $\bar{V}^2$ $\overline{\text{MHV}}$ vertices.[6]

Starting with expression (5.1) for the box graph, it is immediately apparent that the momentum routing through the $\bar{V}^2$s yields the two box-like topologies in LCYM: one with the internal helicities arranged in a clockwise sense (from the first term in the curly braces, shown in figure 9a), and another with an anticlockwise arrangement.

The triangle MHV completion graphs of figure 6 reveal a mixture of topologies in the momentum routing. Naturally, one would expect the triangle diagram of figure 9b, and indeed this arises from the factor Y in (5.19). The MHV completion triangle graph also has terms with factors of X, which we know is nothing but one of the vertex configurations

---

[5]A quick way to generate figure 7a is to note that it can be formed by replacing the product of two three-point Ξs in each term in (5.16) with a single four-point Ξ having the relevant arguments.

[6]Recall that these are the same as the $++-$ vertices in light-cone Yang-Mills.
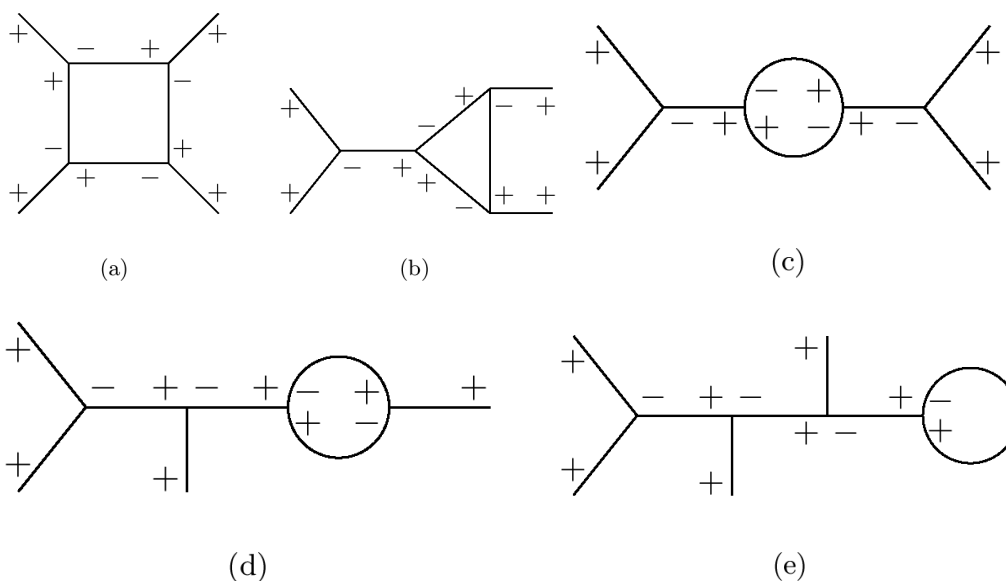
Figure 9: Typical LCYM Feynman graphs that contribute to the $(++++)$ amplitude. Shown topologies are the (a) box, (b) triangle, (c) bubble, (d) typical external leg correction, and (e) one of the tadpoles (there is another tadpole not shown here with the loop attached to the central leg of the tree instead).

in (5.1) of box topology, i.e. figure 9a. (As we have seen however, in this case the fourth propagator is missing.)

The bubble and tadpole graphs can be processed in a similar manner: the graph of figure 7a contains the topology of, and therefore contributes to the reconstruction of, the LCYM self-energy correction graph in figure 9c; similarly figure 7b contributes to the reconstruction of the external leg corrections (an example of which is seen in figure 9d). The MHV completion tadpole graphs in figure 8 contain terms of topology of the LCYM tadpoles of figure 9e (these are ill-defined but we can take them to vanish in dimensional regularisation just as we would for the LCYM tadpole), as well as contributing pieces with the self-energy and external leg correction topologies. Additionally, both MHV completion bubbles and tadpoles contribute to the reconstruction of box and triangle LCYM graphs.

5.5 Full reconstruction of the light-cone Yang-Mills box contribution

Although none of the integrands we have been discussing up to now are identical to the contributions one obtains directly from light-cone Yang-Mills (as a result of Σ_i factors and in all cases except (5.1), missing propagators) we now show that these *are* exactly reproduced when all the contributions of the correct LCYM topology are summed together.

Rather than do this for all graphs displayed in figure 9, we will concentrate on the diagrams of box topology with the internal helicity configuration as displayed in figure 9a. This corresponds to terms containing the factor X in (5.18).

We have already seen that the MHV completion box graph figure 5 provides, through (5.1), the term

$$4g^4 \int \frac{d^D q}{(2\pi)^D} \frac{XC}{q_1^2 q_2^2 q_3^2 q_4^2} \tag{5.22}$$

which is identical to the LCYM box contribution, save for the factor C which is

$$C_{\text{box}} = \frac{P_1 P_2 P_3 P_4}{\Sigma_1 \Sigma_2 \Sigma_3 \Sigma_4}. \tag{5.23}$$

Here we have introduced the short-hand $P_i \equiv p_i^2/\hat{i}$. Similarly from the two triangle configurations in figure 6, we can read off the X terms in (5.17), resulting in (5.22) with C given by

$$C_{\text{triangle}} = \frac{P_2 P_3}{\Sigma_2 \Sigma_3} \frac{Q_4}{\Sigma_4 + \Sigma_1} \left(\frac{P_1}{\Sigma_4} - \frac{P_4}{\Sigma_1} \right). \tag{5.24}$$

Here we have introduced the short-hand $Q_i \equiv q_i^2/\hat{i}$. The presence of Q_4 above is responsible for the missing propagator in this contribution. As we remarked earlier, the bubble diagrams of the form of figure 7a follow straightforwardly by replacing the right half of the diagram of figure 6 by terms corresponding to the left hand half. Thus the four configurations for these bubbles sum to give (5.22) with

$$C_{2|2} = \frac{Q_2}{\Sigma_2 + \Sigma_3} \left(\frac{P_3}{\Sigma_2} - \frac{P_2}{\Sigma_3} \right) \frac{Q_4}{\Sigma_4 + \Sigma_1} \left(\frac{P_1}{\Sigma_4} - \frac{P_4}{\Sigma_1} \right). \tag{5.25}$$

The contributions from the three configurations of bubble, figure 7b, and tadpole, figure 8, are more tedious to derive. We find

$$C_{3|1} = \frac{P_1}{\Sigma_1} \frac{Q_2 Q_3}{\Sigma_2} \left\{ \frac{P_2}{(\Sigma_3 + \Sigma_4)\Sigma_4} - \frac{P_2 + P_3}{(\Sigma_2 + \Sigma_3)\Sigma_4} + \frac{P_2 + P_3 + P_4}{(\Sigma_2 + \Sigma_3)(\Sigma_2 + \Sigma_3 + \Sigma_4)} \right\} \tag{5.26}$$

and

$$C_{\text{tadpole}} = \frac{Q_1 Q_2 Q_3}{\Sigma_1} \left\{ \frac{1}{(\Sigma_1 + \Sigma_2)(\Sigma_1 + \Sigma_2 + \Sigma_3)} - \frac{P_1}{(\Sigma_2 + \Sigma_3 + \Sigma_4)(\Sigma_3 + \Sigma_4)\Sigma_4} \right.$$
$$\left. + \frac{P_1 + P_2}{(\Sigma_1 + \Sigma_2)(\Sigma_3 + \Sigma_4)\Sigma_4} - \frac{P_1 + P_2 + P_3}{(\Sigma_1 + \Sigma_2)(\Sigma_1 + \Sigma_2 + \Sigma_3)\Sigma_4} \right\} \tag{5.27}$$

Now note that, although there is just the one box contribution (5.23), there are four triangle contributions of the form (5.24) obtained by cyclically permuting the labels (corresponding to the four cyclic configurations of external momenta). Similarly there are four cyclic permutations of (5.26) and (5.27) and two of (5.25). Adding all these contributions together, after some tedious but straightforward algebra, one finds that these sum up to $C = 1$. In other words, precisely the light-cone Yang-Mills box contribution is recovered by summing up all of the MHV completion contributions of this topology.

It follows immediately that we obtain the correct on-shell limit of this amplitude (5.15) in D dimensions. However, note well that we have obtained precisely the standard box contribution even before we take the on-shell limit or perform any integration. The recovery

is purely an algebraic process; the MHV completion contributions are nothing but the missing amplitudes from LCYM, rearranged.

In section 5, we obtained the correct standard four-cut contribution by cutting the internal momenta first and only then taking the external momenta on shell. We see again from the contributions above, that taking the limits in this order, only the box (5.23) makes a contribution. However, since the equality is algebraic, the same result is obtained in whatever order one takes the limits.[7] Indeed, if one lets the external momenta go on shell first, then only the tadpole (5.27) makes a contribution, namely

$$C = \frac{Q_1 Q_2 Q_3}{(Q_1 - Q_4)(Q_2 - Q_4)(Q_3 - Q_4)}. \tag{5.28}$$

Adding the three cyclic permutations to this, of course one finds, after simplification, that $C = 1$ again. The tadpole survives this limit because the four different Ξ^s from the four different configurations in figure 8 all provide, upon expansion with (4.25), the same six-point $\Upsilon(q^A, -q^A, 1, 2, 3, 4)$. By (4.21) this has in the denominator a term which cancels the sum over external inverse propagators arising from LSZ reduction:

$$\Omega_q + \Omega_{-q} + \sum_{i=1}^{4} \Omega_i = -\frac{1}{2} \sum_{i=1}^{4} P_i$$

(where momentum conservation and (A.5) have been used).

In fact it is easy to derive the contribution (5.28) in this limit. In (4.21), we keep only the terms in which each factor depends on the loop momentum q, since any factor independent of q corresponds to a tree-level decoration and thus does not have LCYM box topology. However, only the last term satisfies this and thus for the box topology, or more generally the n-gonal topology generated by an n-point tadpole, we can make the replacement

$$\Upsilon(q_n^A, -q^A, 1, \ldots, n) \rightarrow -\frac{\bar{V}^2(-q_{n-1}^B, n, q_n^A) \Upsilon(q_{n-1}^B, -q^A, 1, \ldots, n-1)}{\hat{q}_n(\Omega_{q_n} - \Omega_q + \sum_{i=1}^{n} \Omega_i)}.$$

Iterating this starting with $n = 4$, and recalling the missing propagators, one readily obtains (5.28) and the corresponding term in (5.27).

6. Discussion and conclusions

We have found that amplitudes which are missing from the CSW rules arise in this framework as a result of S-matrix equivalence theorem evasion by the field transformation. We showed this first by calculating the tree-level $(-++)$ amplitude, which is non-vanishing in $(2,2)$ signature/complex momentum. The corresponding vertex, $\bar{V}^2$, is the term that we eliminate from the lagrangian in going from LCYM to one that furnishes CSW rules.

We recovered it via (3.4) by computing the LSZ reduction of the associated correlation function $\langle A\bar{A}\bar{A}\rangle$. Since we have obtained A and $\bar{A}$ as series in B and $\bar{B}$, we calculated this

---

[7]Providing of course one takes the limits in the same order in each term.

correlation function graphically by defining "MHV completion vertices" (so-called since they allow the construction of amplitudes that cannot be built from MHV vertices) for the series coefficients, Υ and Ξ. This correlation function was shown to have divergences in the external momenta, such that it was *not* annihilated when these were taken on shell. The result, even before taking the on-shell limit, correctly reproduces the three-gluon $\overline{\text{MHV}}$ amplitude.

The fact that this missing amplitude is reproduced in the correct form even off shell, is no accident. As we intimated in section 4, we have to recover these terms independently of the form of the eliminated vertex $\bar{V}^2$. Indeed, if we repeat the exercise in the notation of section 4, the equation for the $(++-)$ amplitude is simply

$$\frac{\hat{3}}{2}\left(\sum_{i=1}^{3}\frac{p_i^2}{\hat{i}}\right)\Upsilon(3^K1^I2^J)\left(-\frac{ig}{\sqrt{2}}\right) = \left(-\frac{ig}{\sqrt{2}}\right)\bar{V}^2(1^I2^J3^K),$$

where we have used (A.5) and (4.18). The vertex and the amplitude are thus recovered off shell in D dimensions, whatever its form.

Although we will not do so here, it is clear that we can recover in this way all the discarded tree-level amplitudes, including those illustrated in figure 1. Although these amplitudes vanish on shell, they obviously contribute to off-shell processes such as sub-processes in Standard Model contributions, for example attached to heavy quarks, or at finite virtuality from attaching to hadron wavefunctions. The simple form for the eqs. (2.19) and (2.20) suggests that these off-shell amplitudes also take simple forms in this formalism, just as the on-shell amplitudes do.

It is also the case that the amplitudes in figure 1 no longer vanish in D dimensions, and this is important in recovering the missing one-loop amplitudes. Otherwise, the three-particle and two-particle cuts of the LCYM box contribution, figure 9a would vanish on shell, in contradiction with the known answer (5.15).

Recall that we have seen that the algebraic equivalence between the formalism we have presented here and the LCYM theory, extends also to the quantum level. The exact one-loop LCYM box contribution to the $(++++)$ amplitude was recovered from the diagrams constructed from the Ξ MHV completion vertices before taking any limits or performing the loop momentum integration. The contributions that sum to these 'lost' amplitudes are readily recognised by expressing them in terms of $\bar{V}^2$ and using these to extract the relevant topologies. Although we concentrated on this one topology it is clear that all the topologies in figure 9 will be recovered in this way.

In order for the quantum corrections we have been discussing to be well defined we need to incorporate a regularisation scheme for MHV diagrams. We augmented the usual light-cone co-ordinates in a manner that allows us to preserve the ideas of positive and negative 'helicity' and hence apply the canonical transform to all the degrees of freedom outside four dimensions. The series solution to this change of variables follows in a manner similar to the four-dimensional case, but the results are not as simple. In particular, we do not have all orders compact holomorphic expressions for the series coefficients or for the generalisations of the tree-level MHV rules. However we do gain a lagrangian containing

only MHV interactions with two negative helicities and any number of positive helicities. As in the four dimensional case, this has the consequence of imposing an MHV rules 'grading' on perturbation theory so that in particular at tree level and one loop, only amplitudes with two or more negative helicities can be created by sewing together lagrangian vertices. We inherit its simplicity in the sense that at tree-level the first non-vanishing amplitudes are MHV amplitudes, these coinciding with the lagrangian vertices, that NMHV amplitudes are constructed by joining precisely two such vertices together by the propagator and so on.

We used this regularisation to study in detail the standard cuts of the MHV completion box contribution (of figure 5) to $(++++)$ amplitude, i.e. the generalised unitarity cuts that follow from cutting the propagators. If we leave the external momenta off shell until after the internal propagators are cut, then we find that only its quadruple cut is non-zero. As we noted, it is clear immediately from the expression in terms of $\bar{V}^2$ that this is the quadruple cut of the LCYM box contribution. Nevertheless, we computed it in full and confirmed that it agreed with the known result for the full amplitude. This is supporting evidence that the dimensional regularisation we have put in place is indeed consistent. It also allowed us to demonstrate that the solution for the cuts can be obtained directly in terms of the bilinear brackets (4.2), which play the rôle of D dimensional generalisations of the familiar spinor brackets.

On the other hand the other diagrams we can make, *cf.* figures 6–8, evaluated this way, have no standard four-cut contributions. In general which diagrams contribute depends on the way in which we take the on-shell limit. For example, we saw that if we take the external momenta on shell first, before cutting the diagram, then only the tadpole contributions in figure 8 contribute. In this case these alone sum to provide the LCYM box contribution. Since the sum total of the contributions from all diagrams is just equal to that of LCYM, before integration, we are free to choose how we take the on-shell limits.

Although we have not treated the higher-point all-+ amplitudes, we have no doubt that they would be recovered by the methods above.

In general, by computing all the standard cuts outside four dimensions we can reconstruct the amplitude, on or off shell, without unfolding back to LCYM. This follows by noting that it is just these cuts of propagators that enters the Feynman tree theorem [31].

Another possibility to be further explored is the direct evaluation of integrals such as (5.1). So far, we have just assumed that the integrals corresponding to individual contributions exist and either matched their properties to known functions or recognised that summing them gives back previously treated amplitudes. However, direct evaluation presents a number of technical challenges, in particular providing the correct treatment of the non-standard cuts arising from the singularity surfaces incorporated in the Υ and Ξ vertices.

To summarise, we can conclude that the canonical MHV lagrangian, supplemented as required by the Υ and Ξ coefficients as in (3.3), merely rearranges LCYM theory: the full evaluation of any such amplitude recovers precisely the original LCYM amplitudes. Of course it is important here that the canonical transformation to the MHV lagrangian has unit jacobian both in four and D dimensions. The fact that we do recover the LCYM

contributions at one loop in such a straightforward way, gives us confidence in assuming that the jacobian is anomaly free (contrary to speculations in the literature that such an anomaly might be responsible for the $(++++)$ amplitude).

Although we have concentrated on the rôle of the Υ and Ξ vertices in evading the equivalence theorem, we see that they are important in general for recovering the correct off shell structure. For example by incorporating these, renormalisation of the canonical MHV lagrangian is as straightforward (or indeed as problematic [53]) as renormalising LCYM.

We have seen that these vertices are required for some on-shell amplitudes. Presumably they are not required for some amplitudes where only certain legs are off shell. We leave for the future determining precisely when we need to utilise the Υ and Ξ vertices in any given amplitude.

It is clear that we can perform canonical transformations to eliminate interactions from other lagrangians, employing light cone coordinates, generalising (2.14), and in so doing arrive at generalised versions of canonical MHV lagrangians. For example we can apply this technique to other parts of the Standard Model. Since the recovery of the missing amplitudes by including the Υ and Ξ vertices works whatever the form of $\bar{V}^2(1^I 2^J 3^K)$, this mechanism will function equally well for these generalisations (even where higher-point interactions have been subsumed). We leave as a subject of future research the question of whether such generalisations, and indeed the MHV framework for Yang-Mills applied in more generality as we have been discussing, lead to sufficiently simpler computations compared to standard methods.

Acknowledgments

Note added: after this paper was completed ref. [60] appeared which addresses these issues from a different perspective.

A. Light-cone vector identities

The appendix gives some of the identities particular to vectors in D-dimensional light-cone co-ordinates. Some of these appear in a different form in [61]. First, for any two D-vectors p and q,

$$(p\,q)\cdot\{p\,q\} = -\frac{1}{2}(\hat{p}\,q - \hat{q}\,p)^2 \tag{A.1}$$

from which it is clear that for null p, q,

$$(p\,q)\cdot\{p\,q\} = \hat{p}\,\hat{q}\,p\cdot q. \tag{A.2}$$

The Bianchi-like identity

$$\hat{i}(j\,k) + \hat{j}(k\,i) + \hat{k}(i\,j) = 0 \tag{A.3}$$

holds also under replacement of the hat with any transverse component i_I or $\bar{i}_I$, and replacement of the bilinear with its adjoint.

For a set of momenta $\{p_j\}$ that sum to zero,

$$\sum_j \frac{(p\,j)\cdot\{j\,q\}}{\hat{j}} = \frac{\hat{p}\hat{q}}{2}\sum_j \frac{p_j^2}{\hat{j}} \tag{A.4}$$

for any p and q. This is the D-dimensional, off-shell generalisation of the spinor identity $\sum_j \langle p\,j\rangle[j\,q] = \langle p|(\sum_j |j\rangle[j|)|q] = 0$. In four dimensions the above identity looks the same except that the dot product is simply multiplication. Also,

$$\sum_j \Omega_j = -\frac{1}{2}\sum_j \frac{p_j^2}{\hat{j}}. \tag{A.5}$$

(In four dimensions the left hand side has ω_j in place of Ω_j.)

References

[1] S.J. Parke and T.R. Taylor, *An amplitude for n gluon scattering*, *Phys. Rev. Lett.* **56** (1986) 2459.

[2] F.A. Berends and W.T. Giele, *Multiple soft gluon radiation in parton processes*, *Nucl. Phys.* **B 313** (1989) 595.

[3] S. J. Parke and M. L. Mangano, *The structure of gluon radiation in QCD*, FERMILAB-CONF-89-180-T, Invited talk at the Workshop on QED Structure Functions, Ann Arbor, MI, May 22-25 (1989).

[4] E. Witten, *Perturbative gauge theory as a string theory in twistor space*, *Commun. Math. Phys.* **252** (2004) 189 [hep-th/0312171].

[5] F. Cachazo, P. Svrcek and E. Witten, *Mhv vertices and tree amplitudes in gauge theory*, *JHEP* **09** (2004) 006 [hep-th/0403047].

[6] G. Georgiou and V.V. Khoze, *Tree amplitudes in gauge theory as scalar MHV diagrams*, *JHEP* **05** (2004) 070 [hep-th/0404072].

[7] J.-B. Wu and C.-J. Zhu, *MHV vertices and scattering amplitudes in gauge theory*, *JHEP* **07** (2004) 032 [hep-th/0406085].

[8] I. Bena, Z. Bern and D.A. Kosower, *Twistor-space recursive formulation of gauge theory amplitudes*, *Phys. Rev.* **D 71** (2005) 045008 [hep-th/0406133].

[9] J.-B. Wu and C.-J. Zhu, *MHV vertices and fermionic scattering amplitudes in gauge theory with quarks and gluinos*, *JHEP* **09** (2004) 063 [hep-th/0406146].

[10] D.A. Kosower, *Next-to-maximal helicity violating amplitudes in gauge theory*, *Phys. Rev.* **D 71** (2005) 045007 [hep-th/0406175].

[11] G. Georgiou, E.W.N. Glover and V.V. Khoze, *Non-MHV tree amplitudes in gauge theory*, *JHEP* **07** (2004) 048 [hep-th/0407027].

[12] R. Britto, F. Cachazo, B. Feng and E. Witten, *Direct proof of tree-level recursion relation in Yang-Mills theory*, *Phys. Rev. Lett.* **94** (2005) 181602 [hep-th/0501052].

[13] K. Risager, *A direct proof of the CSW rules*, *JHEP* **12** (2005) 003 [hep-th/0508206].

[14] R. Britto, F. Cachazo and B. Feng, *New recursion relations for tree amplitudes of gluons*, *Nucl. Phys.* **B 715** (2005) 499 [hep-th/0412308].

[15] R. Britto, B. Feng, R. Roiban, M. Spradlin and A. Volovich, *All split helicity tree-level gluon amplitudes*, *Phys. Rev.* **D 71** (2005) 105017 [hep-th/0503198].

[16] Z. Bern, G. Chalmers, L.J. Dixon and D.A. Kosower, *One loop n gluon amplitudes with maximal helicity violation via collinear limits*, *Phys. Rev. Lett.* **72** (1994) 2134 [hep-ph/9312333].

[17] G. Mahlon, *Multi-gluon helicity amplitudes involving a quark loop*, *Phys. Rev.* **D 49** (1994) 4438 [hep-ph/9312276].

[18] Z. Bern, L.J. Dixon and D.A. Kosower, *On-shell recurrence relations for one-loop QCD amplitudes*, *Phys. Rev.* **D 71** (2005) 105013 [hep-th/0501240].

[19] C.F. Berger, Z. Bern, L.J. Dixon, D. Forde and D.A. Kosower, *All one-loop maximally helicity violating gluonic amplitudes in QCD*, *Phys. Rev.* **D 75** (2007) 016006 [hep-ph/0607014].

[20] R. Britto, F. Cachazo and B. Feng, *Computing one-loop amplitudes from the holomorphic anomaly of unitarity cuts*, *Phys. Rev.* **D 71** (2005) 025012 [hep-th/0410179].

[21] Z. Bern, L.J. Dixon and D.A. Kosower, *Bootstrapping multi-parton loop amplitudes in QCD*, *Phys. Rev.* **D 73** (2006) 065013 [hep-ph/0507005].

[22] Z. Bern, L.J. Dixon, D.C. Dunbar and D.A. Kosower, *Fusing gauge theory tree amplitudes into loop amplitudes*, *Nucl. Phys.* **B 435** (1995) 59 [hep-ph/9409265].

[23] A. Brandhuber, S. McNamara, B.J. Spence and G. Travaglini, *Loop amplitudes in pure Yang-Mills from generalised unitarity*, *JHEP* **10** (2005) 011 [hep-th/0506068].

[24] Z. Bern, L.J. Dixon and D.A. Kosower, *The last of the finite loop amplitudes in QCD*, *Phys. Rev.* **D 72** (2005) 125003 [hep-ph/0505055].

[25] Z. Bern, N.E.J. Bjerrum-Bohr, D.C. Dunbar and H. Ita, *Recursive calculation of one-loop QCD integral coefficients*, *JHEP* **11** (2005) 027 [hep-ph/0507019].

[26] C.F. Berger, Z. Bern, L.J. Dixon, D. Forde and D.A. Kosower, *Bootstrapping one-loop QCD amplitudes with general helicities*, *Phys. Rev.* **D 74** (2006) 036009 [hep-ph/0604195].

[27] F. Cachazo, P. Svrcek and E. Witten, *Twistor space structure of one-loop amplitudes in gauge theory*, *JHEP* **10** (2004) 074 [hep-th/0406177].

[28] F. Cachazo, P. Svrcek and E. Witten, *Gauge theory amplitudes in twistor space and holomorphic anomaly*, *JHEP* **10** (2004) 077 [hep-th/0409245].

[29] F. Cachazo, *Holomorphic anomaly of unitarity cuts and one-loop gauge theory amplitudes*, hep-th/0410077.

[30] A. Brandhuber, B.J. Spence and G. Travaglini, *One-loop gauge theory amplitudes in $N = 4$ super Yang-Mills from MHV vertices*, *Nucl. Phys.* **B 706** (2005) 150 [hep-th/0407214].

[31] A. Brandhuber, B. Spence and G. Travaglini, *From trees to loops and back*, *JHEP* **01** (2006) 142 [hep-th/0510253].

[32] Z. Xiao, G. Yang and C.-J. Zhu, *The rational part of QCD amplitude. I: the general formalism*, *Nucl. Phys.* **B 758** (2006) 1 [hep-ph/0607015].

[33] J. Bedford, A. Brandhuber, B.J. Spence and G. Travaglini, *Non-supersymmetric loop amplitudes and MHV vertices*, *Nucl. Phys.* **B 712** (2005) 59 [hep-th/0412108].

[34] R. Britto, F. Cachazo and B. Feng, *Generalized unitarity and one-loop amplitudes in $N = 4$ super-Yang-Mills*, *Nucl. Phys.* **B 725** (2005) 275 [hep-th/0412103].

[35] S.J. Bidder, N.E.J. Bjerrum-Bohr, D.C. Dunbar and W.B. Perkins, *One-loop gluon scattering amplitudes in theories with $N < 4$ supersymmetries*, *Phys. Lett.* **B 612** (2005) 75 [hep-th/0502028].

[36] E.I. Buchbinder and F. Cachazo, *Two-loop amplitudes of gluons and octa-cuts in $N = 4$ super Yang-Mills*, *JHEP* **11** (2005) 036 [hep-th/0506126].

[37] K. Risager, S.J. Bidder and W.B. Perkins, *One-loop NMHV amplitudes involving gluinos and scalars in $N = 4$ gauge theory*, *JHEP* **10** (2005) 003 [hep-th/0507170].

[38] Z. Bern, L.J. Dixon and D.A. Kosower, *All next-to-maximally helicity-violating one-loop gluon amplitudes in $N = 4$ super-Yang-Mills theory*, *Phys. Rev.* **D 72** (2005) 045014 [hep-th/0412210].

[39] C. Quigley and M. Rozali, *One-loop MHV amplitudes in supersymmetric gauge theories*, *JHEP* **01** (2005) 053 [hep-th/0410278].

[40] J. Bedford, A. Brandhuber, B.J. Spence and G. Travaglini, *A twistor approach to one-loop amplitudes in $N = 1$ supersymmetric Yang-Mills theory*, *Nucl. Phys.* **B 706** (2005) 100 [hep-th/0410280].

[41] A. Gorsky and A. Rosly, *From Yang-Mills lagrangian to MHV diagrams*, *JHEP* **01** (2006) 101 [hep-th/0510111].

[42] P. Mansfield, *The lagrangian origin of MHV rules*, *JHEP* **03** (2006) 037 [hep-th/0511264].

[43] M.C. Bergere and Y.-M.P. Lam, *Equivalence theorem and Faddeev-Popov ghosts*, *Phys. Rev.* **D 13** (1976) 3247.

[44] G. Chalmers and W. Siegel, *The self-dual sector of QCD amplitudes*, *Phys. Rev.* **D 54** (1996) 7628 [hep-th/9606061].

[45] C. Itzykson and J. B. Zuber, *Quantum Field Theory*, New York, McGraw-Hill (1980).

[46] J.H. Ettle and T.R. Morris, *Structure of the MHV-rules lagrangian*, *JHEP* **08** (2006) 003 [hep-th/0605121].

[47] H. Feng and Y.-t. Huang, *Mhv lagrangian for $N = 4$ super Yang-Mills*, hep-th/0611164.

[48] A. Brandhuber, B. Spence and G. Travaglini, *Amplitudes in pure Yang-Mills and MHV diagrams*, *JHEP* **02** (2007) 088 [hep-th/0612007].

[49] L.J. Mason and D. Skinner, *An ambitwistor Yang-Mills lagrangian*, *Phys. Lett.* **B 636** (2006) 60 [hep-th/0510262].

[50] R. Boels, L. Mason and D. Skinner, *Supersymmetric gauge theories in twistor space*, *JHEP* **02** (2007) 014 [hep-th/0604040].

[51] R. Boels, L. Mason and D. Skinner, *From twistor actions to MHV diagrams*, *Phys. Lett.* **B 648** (2007) 90 [hep-th/0702035].

[52] R. Boels, *A quantization of twistor Yang-Mills theory through the background field method*, `hep-th/0703080`.

[53] G. Leibbrandt, *The light cone gauge in Yang-Mills theory*, *Phys. Rev.* **D 29** (1984) 1699.

[54] R.J. Eden, P.V. Landshoff, D.I. Olive and J.C. Polkinghorne, *The analytic S-matrix*, Cambridge University Press (1966).

[55] R.P. Feynman, *Closed loop and tree diagrams*, in *J. R. Klauder, Magic Without Magic*, San Francisco (1972).

[56] L.J. Dixon, *Calculating scattering amplitudes efficiently*, `hep-ph/9601359`.

[57] Z. Bern, L.J. Dixon and D.A. Kosower, *One loop corrections to five gluon amplitudes*, *Phys. Rev. Lett.* **70** (1993) 2677 [`hep-ph/9302280`].

[58] Z. Bern, L.J. Dixon and D.A. Kosower, *New QCD results from string theory*, `hep-th/9311026`.

[59] Z. Bern and A.G. Morgan, *Massive loop amplitudes from unitarity*, *Nucl. Phys.* **B 467** (1996) 479 [`hep-ph/9511336`].

[60] A. Brandhuber, B. Spence, G. Travaglini and K. Zoubos, *One-loop MHV Rules and Pure Yang-Mills*, `hep-th/0704.0245`.

[61] D. Chakrabarti, J. Qiu and C.B. Thorn, *Scattering of glue by glue on the light-cone worldsheet. I: helicity non-conserving amplitudes*, *Phys. Rev.* **D 72** (2005) 065022 [`hep-th/0507280`].